energies

MDPI

Review

Review of Film Cooling in Gas Turbines with an Emphasis on Additive Manufacturing-Based Design Evolutions

Sandip Dutta [1,*], Inderjot Kaur [2] and Prashant Singh [3]

[1] Department of Mechanical Engineering, Clemson University, Clemson, SC 29634, USA
[2] Department of Mechanical Engineering, Mississippi State University, Starkville, MS 39762, USA
[3] Mechanical, Aerospace, and Biomedical Engineering, University of Tennessee, Knoxville, TN 37996, USA
* Correspondence: sdutta@clemson.edu

Abstract: Film-cooling technology is used in high-temperature components of gas turbines to extend their service lives. Hot-gas path components are susceptible to damage or failure in the absence of film cooling. Much of the optimization research efforts have been focused on film hole shapes, heat/mass transfer measurement techniques, and film cooling performance under various mainstream and coolant side operating conditions. Due to recent rapid advancements in the areas of measurement techniques (e.g., pressure-sensitive paints and fast high-resolution imaging) and metal additive manufacturing (AM), film cooling technology has undergone significant changes and shows potential new development. In this review, a historical perspective is discussed covering over five decades of innovation: the geometrical effects from injection angle and hole shapes; flow effects from density ratio, momentum-flux ratio, blowing ratio, advective capacity ratio, and freestream conditions; and more items related to AM. The impact of AM on film hole design strategies, the challenges posed by state-of-the-art AM technology, and pathways for future research are discussed. A comparative analysis of AM assisted film hole fabrication and conventionally manufactured film holes is elaborated.

Keywords: film cooling; additive manufacturing; heat transfer; gas turbine

Citation: Dutta, S.; Kaur, I.; Singh, P. Review of Film Cooling in Gas Turbines with an Emphasis on Additive Manufacturing-Based Design Evolutions. *Energies* **2022**, *15*, 6968. https://doi.org/10.3390/en15196968

Academic Editor: Jian Liu

Received: 3 August 2022
Accepted: 15 September 2022
Published: 23 September 2022

1. Introduction

This paper is expanded from an ASME conference paper by the same set of authors (Kaur et al. [1]). The film cooling concept has been scientifically analyzed since the 1970s, even though the first successful gas turbine was demonstrated in Paris in 1903. The reason behind this delay in film cooling innovation is that in the beginning, turbine design focused more on aerodynamics, vibration and noise, and combustion stability. As the operating temperature of gas turbines increased to improve thermal efficiency, this cooling technique became critical for the success of turbine operations, and because of its crucial role, high-temperature real engine-cooling design correlations can be treated as protected national intellectual property in the US or other countries that are capable of developing aerospace and missile technologies. Modern-day gas turbine components are exposed to mainstream flow temperatures as high as 1700 °C, as shown in Figure 1, and the trend is going higher for turbine inlet temperature to obtain better thermal efficiency. High-pressure turbine components are subjected to an extremely hostile environment with the exposure to the combustor exit, which imposes high thermal loads on the exposed surfaces. Longevity of operation can be ensured only if the temperature of the components is maintained below the recommended operating limits of these materials, which are usually a combination of metals and ceramics. In addition to these steady-state thermal loads, there are startup, shutdown, and loading variations, which significantly affect the turbine's durability. Turbine manufacturers frequently develop two product lines: one is made for steady-state high-efficiency (Carnot cycle-based high temperature) continuous operations,

and the other is the Peaker turbine, which can ramp up to produce power quickly when there is a peak in demand and shut down when the demand is low. In addition, there are part-load turbines that can operate for long hours at a fraction of the full load. Various cooling concepts have been proposed by researchers in the turbomachinery community to keep the surface temperatures within permissible limits, and film cooling (FC) is one such disruptive technology introduced in the 1970s. Recent progress in additive manufacturing (AM) is bringing the need for new analysis, as demonstrated by Bogard et al. [2]. Note that cooling procedures reduce the thermal efficiency of the turbine and are considered necessary evils. The film cooling is especially bad on aerodynamic performance because it interferes with the hot gas flow. However, to achieve the higher operating temperatures, FC has not found an alternative yet. Evolution of a new ceramic–matrix composite (CMC) provides opportunities to operate the turbine at 3000 °C [3]. The CMC can tolerate high temperature, but does not respond well to moisture, so there are inherent unresolved challenges in its adoption. However, with CMC technology maturation for employment in complex turbine parts, FC may not be needed on those components [4]. There is an ongoing effort to produce CMC components with the emerging additive manufacturing technologies [5]. The changes in film cooling from AM are akin to evolution (gradual), as opposed to revolutionary major breakthroughs.

Film cooling involves the introduction of a coolant through one or more discrete locations on an exposed surface such that the ejected fluid hugs the surface and forms a protective layer (a.k.a. film) between the surface and the hot mainstream gases. Fluid ejected through a continuous slot that runs transversely across the exposed wall is ideal, because of the uniform spread of the coolant layer it provides on the surface, but the structural integrity of the critical turbine components, such as blades, as well as the amount of coolant needed to cover the entire surface, can be prohibitive for an economical design. Instead of full coverage, injection of the coolant through discrete holes with their exits flushed against the surface is preferred. Goldstein [6] provided a comprehensive review of the continuous slot- and discrete hole-type configurations. An early explorer of this cooling technique, Goldstein highlighted that the flow field around the coolant ejected from the continuous slots could be treated as two-dimensional, whereas the discrete placement of injection holes resulted in complex three-dimensional flow physics in the regions downstream of hole exits and within span-wise gaps of adjacent holes in a row. This rendered the development of analytical models for predicting thermal parameters based on 3-D boundary layer analysis in discrete hole configurations very challenging. Several experimental and numerical investigations have been conducted over the last five decades to characterize the film cooling performance of a wide variety of hole shapes for a broad range of flow conditions. Zhang et al. [7] presented a review of recent publications on film cooling. They compiled 150 references related to film cooling and provide a good source to find relevant references. Film cooling in gas turbines involves gas-to-gas interactions, whereas in other applications, such as rocket engines, liquid-to-vapor phase change can be applied in film or wall jets [8]. Rao et al. [9] showed cooling enhancement with mist-assisted film cooling. It is hard to get inside design information from turbine manufacturers, but there are two technical articles released by Mitsubishi Heavy Industries to illustrate their 1600 °C J-series gas turbines [10,11]. These designs showed that film cooling was one of the major techniques needed to achieve such a high operating temperature, as illustrated in Figure 1.

This decade's economic growth is counting on new manufacturing technologies, innovative designs, and optimizations. Figures 2 and 3 show a few samples of additively manufactured whole turbine components and test coupons used for evaluating film cooling performance. Horizon Technology [12] has listed several advantages and disadvantages of additive manufacturing that align with this topic, which are listed in Table 1. Additional aspects of film hole AM manufacturing are that the tool traverse path is not relevant in AM and therefore the hole size and shape can be varied irrespective of the hole location on the component.

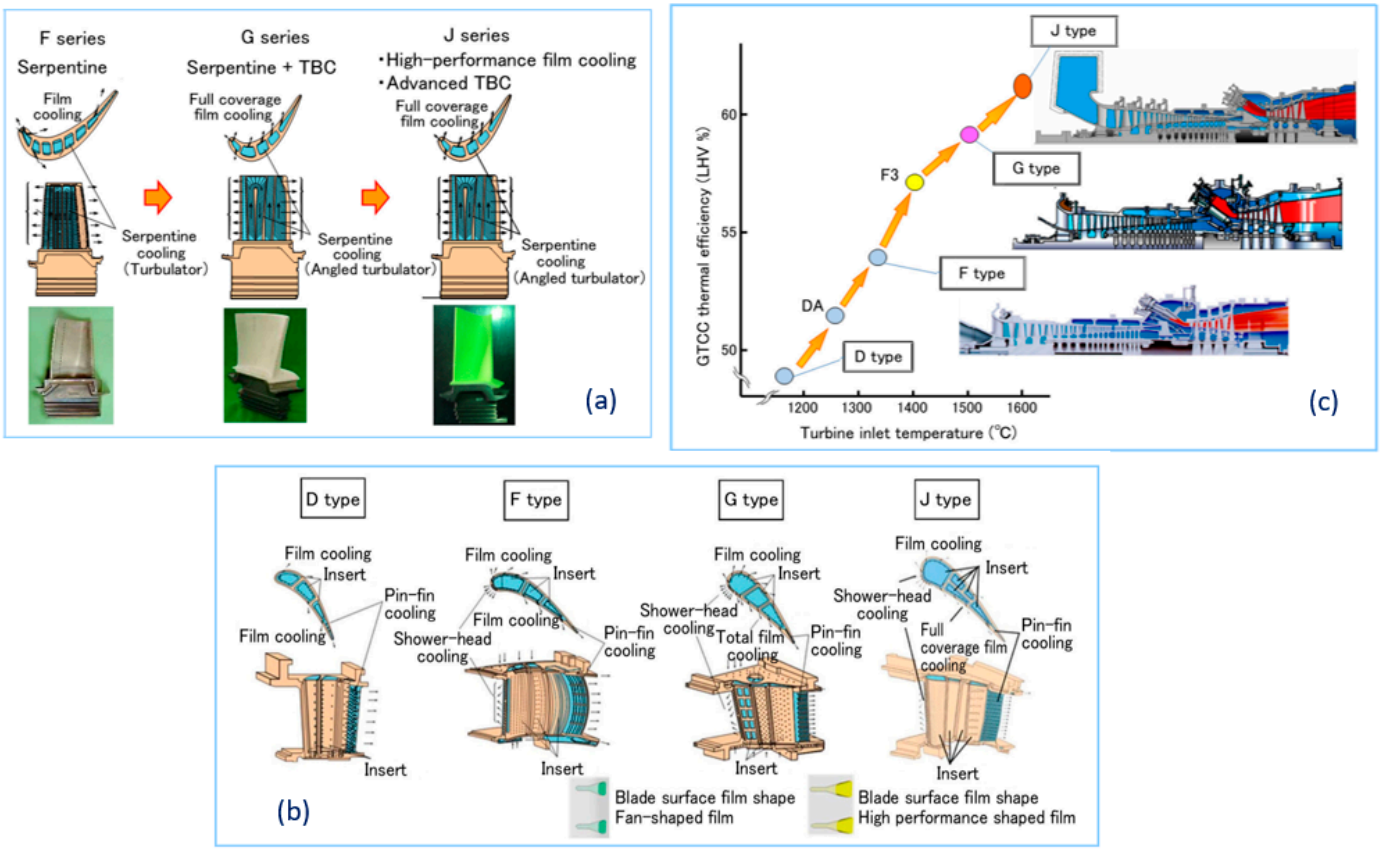

Figure 1. Historical design improvement by Mitsubishi Heavy Industries. Cooling design improvement in (**a**) rotating airfoil and (**b**) stationary airfoil. (**c**) The operating temperature increased as the efficiency increased [10,11].

(**a**) (**b**)

Figure 2. Metal and ceramic turbine blades produced via new manufacturing processes [13,14], and more in [15]. (**a**) Rotor Blades, (**b**) Airfoil with complex cooling features (courtesy: Castheon Inc.)

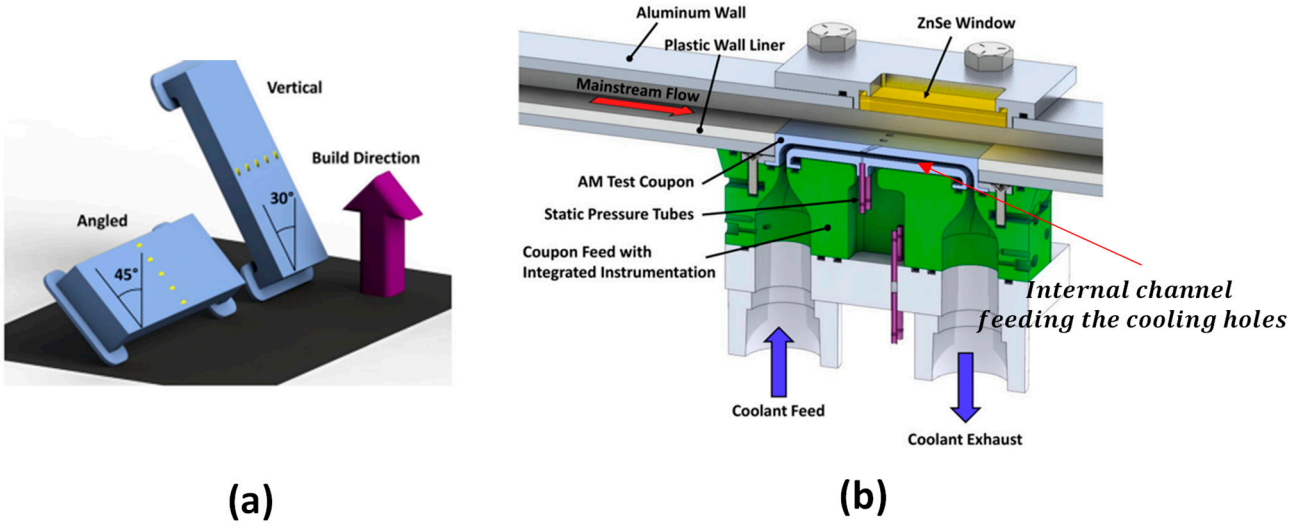

Figure 3. (**a**) Build orientations for coupons, and (**b**) cut-section view of the test rig and the additively manufactured coupons showing the internal channel (which can have either coflow or counterflow direction with respect to mainstream flow) to feed the film cooling holes (Stimpson et al. [16]).

Table 1. Advantages and disadvantages of AM as listed by a manufacturer [12].

AM Advantages	AM Disadvantages
1. Unusual or Complex component shapes can be produced-like hollow spaces, honeycomb or other thin-walled internal structures, internal cooling channels, negative drafts.	1. Part cost from equipment use. Equipment uses high temperature technologies and sophisticated computation technologies. That cost needs to be distributed in different manufactured parts as hourly equipment usage rate.
2. Assembled product is manufactured. Conventional manufacturing separated thick walled and thin-walled structures by different manufacturing processes.	2. Surface finish can be rough and may need additional touchups.
3. No tooling or production line changeover costs. Since all components start with similar raw material and the same tooling, the product change does not involve extensive production line alterations.	3. Dimensional control is challenging as the metal solidification and cooling can create distortions.
	4. Restriction on alloys that are friendly for the AM processes.
	5. Slowness and size limitations exist as the technology is still under development.

FC Variables of interest: Convective thermal load as transferred from hot mainstream gases to the exposed blade surface is given by the following equation:

$$q = h(T_{ref} - T_w) \quad (1)$$

where h is the convective heat transfer coefficient, T_w is the surface temperature and T_{ref} is the reference temperature. In the absence of coolant fluid, the mainstream temperature (T_∞) serves as the reference temperature. In the presence of the film-coolant layer between the hot mainstream gas and the surface, the coolant temperature (T_c) can be intuitively considered the appropriate reference temperature. However, once the coolant fluid is injected into the mainstream, it interacts, diffuses into the mainstream, and gets diluted by the ingestion of the hot mainstream flow. Therefore, the film temperature in the proximity of the surface is different from T_c.

Local wall temperatures in Figure 4 show that the complete film coverage of the surface is usually not feasible [17], even with a slot hole, and as a result, an average of the values of the film effectiveness and h are usually provided. The film coming out can be pulsed, and a study on synthetic jets showed that by controlling the pulsation frequency, local improvement in near-hole or far-hole regions can be achieved [18]. As such, for analyzing film cooled heat loads, an average h is required and usually it is different from the h

obtained without film cooling. LES simulation of converging slot holes was performed by Wang et al. [19], and more details were provided in that article.

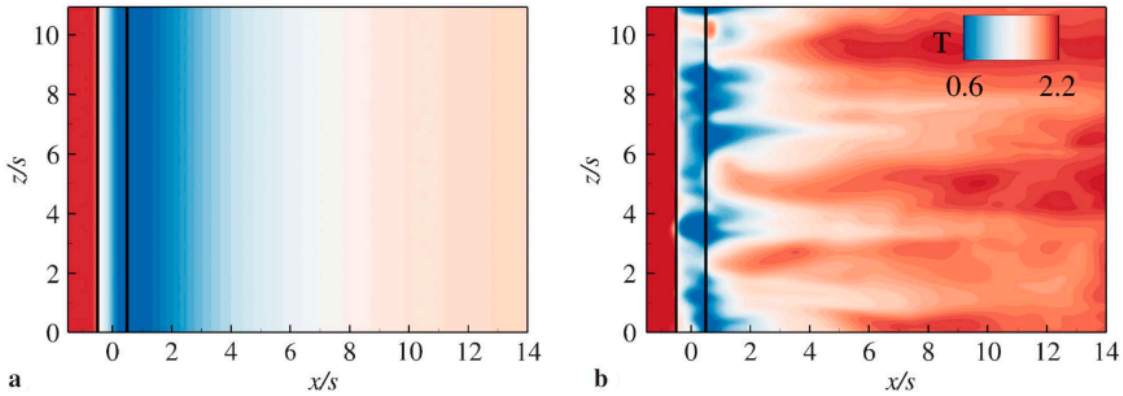

Figure 4. Slot film pattern for (**a**) laminar and (**b**) turbulent flow indicates that film is not really a uniform coverage, but rather forms streaks even if the injection source is a slot. [17]. The plot shows local wall temperatures, blue being cooler than red.

Adiabatic wall temperature (T_{aw}) has been considered the most suitable representative film temperature in complex fluid-mixing scenarios. T_{aw} would prevail over the surface if it were perfectly insulated (zero heat flux). Equation (1) can then be represented as $q = h(T_{aw} - T_w)$, which makes film cooling a three-temperature problem, viz. T_∞, T_c, and T_{aw}. The adiabatic wall temperature is calculated in nondimensional form as film cooling effectiveness (η), as given in Equation (2):

$$\eta = \frac{T_\infty - T_{aw}}{T_\infty - T_c} \tag{2}$$

The footprints of η on surface walls with higher magnitudes (max = 1) over a larger coverage area, both streamwise and spanwise, signify more effective film cooling. The turbulence generated by the mixing of the ejected coolant, vortex creation, and mainstream gas-path disturbances can enhance the heat transfer on the blade surface in comparison to no-film cooling, as given by the following equation:

$$\frac{q}{q_0} = \frac{h(T_{aw} - T_w)}{h_0(T_\infty - T_w)} = \frac{h}{h_0}\left(1 - \eta\frac{T_\infty - T_c}{T_\infty - T_w}\right) \tag{3}$$

The quantity q/q_0 is desired to be less than unity to obtain overall benefit from film cooling; q_0 is the heat flux in the absence of film cooling. The high film effectiveness (η) should not be undermined by the high heat transfer coefficient (h) downstream of the holes. Generally, the overall benefit of film cooling is expressed through net heat flux reduction, given as $(NHFR = 1 - q/q_0)$. Therefore, one needs to determine both parameters h and η to quantify the overall performance of any film cooling configuration.

The investigations reported in film cooling literature have been dedicated to determining either one or both of the variables of interest discussed above (h and η). Quantifiable influences from hole geometry, coolant and mainstream fluid properties, and operating conditions on these film cooling variables have been thoroughly investigated. The following section briefly describes the prominent historical studies in this regard and some recent investigations along with different experimental techniques. More coverage on these FC parameters were provided by Han et al. [20]. The next section focusses on the scope of alternative emerging technology additive manufacturing (AM) in film cooling applications. Detailed discussion is provided on the progress of AM in manufacturing film holes and challenges faced by the state-of-the-art AM technologies in rendering repeatable and reliable data for film cooling. There are several other fluid phenomena that were

observed to affect the film cooling, such as vortex shedding frequency past the film ejected flow [21]. As expected, a higher vortex shedding frequency disturbed the film and reduced its effectiveness.

2. Historical Perspective of Film-Cooling Performance

This section provides a brief description of the developments made in hole design and shape and prominent studies that reported on the influence of coolant and mainstream fluid properties on the overall performance of film cooling holes. The impact of mainstream flow conditions is also discussed, along with experimental measurements techniques that have evolved over the last five decades. Huang et al. [22] performed complex multiobjective shape optimization of fan-shaped holes and, like most researchers, missed a key parameter—the hood over the film hole. There are other parameters that have not been studied in detail, like curved hole shapes as patented by United Technologies [23], where the design showed a significant hood and creative floor designs to disturb the typical vortex formations in film cooling. The counterrotating vortex pair was illustrated by Li et al. [24], where they showed the liftoff and reattachment in film cooling flow. Aminov et al. [25] studied the turbine inlet temperature effects on cycle operation. The turbine inlet temperature is a theoretical estimate of gas temperature that includes the film coolant flows on the upstream stationary components. Film cooling is not only needed for cooling, but also to determine the turbine inlet temperature. Moreover, the uneven distribution of film coolant exit flows can make the flow entering the turbine an uneven temperature and influences the component's life parameters. Chen and Park et al. [26,27] looked at the backward injection of film and found some situations where the opposing film direction can be beneficial. A tabulated summary of film cooling on end walls was provided by Barigozzi et al. [28], so is not repeated here.

2.1. Hole Positioning and Film Exit Configurations

Round film holes with circular metering sections machined at shallow angles relative to the test surface have been the focus of investigation in many earlier studies. The broadscale applicability of such holes is due to the ease in manufacturing through electrodischarge machining (EDM), laser drilling, or water-jet drilling. In 1974, Goldstein [29] introduced the concept of "shaped holes," where the holes had a circular metering region at the entrance of the secondary fluid, but laterally expanded by 10° near the exit. Widening of the exit resulted in better spread of the coolant in directions lateral to the hole centerline, thereby improving the overall coverage of the coolant fluid. Moreover, expansion in flow area reduced the momentum flux at the exit that inhibits the greater penetration of the ejecting coolant jet into the mainstream flow and it stays closer to the surface. Figure 5 shows a few popular film hole shapes. Interestingly, a critical film shape parameter, hood length, has been neglected in the literature. Figure 6 shows a few patented designs for hooded film holes. Figure 7 shows some more variations of the film hole that somewhat tried to capture the hood effect without realizing it. In a hooded film hole, part of the expansion region has a cover.

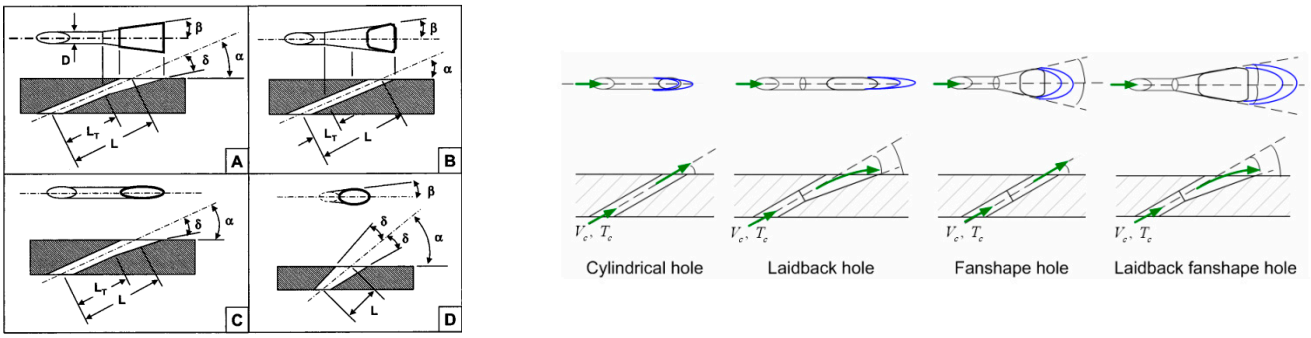

Figure 5. Popular design configurations of film cooling holes [30,31] are schematically illustrated in (**A**–**D**). More configurations are available in [32].

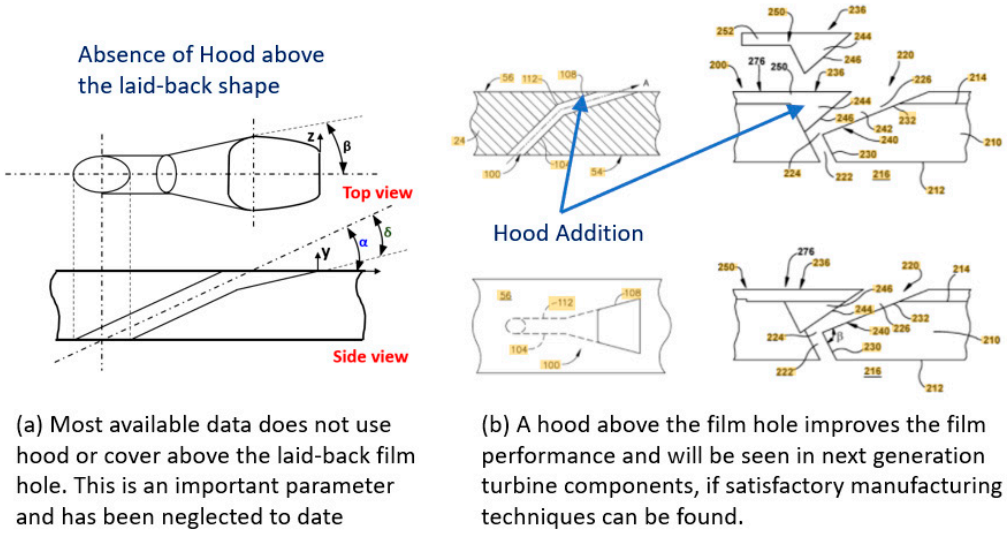

(a) Most available data does not use hood or cover above the laid-back film hole. This is an important parameter and has been neglected to date

(b) A hood above the film hole improves the film performance and will be seen in next generation turbine components, if satisfactory manufacturing techniques can be found.

Figure 6. Patent publications show internal knowledge in the gas turbine industry that film hood has a significant influence on the attachment and stability of the cooling film [22,33,34].

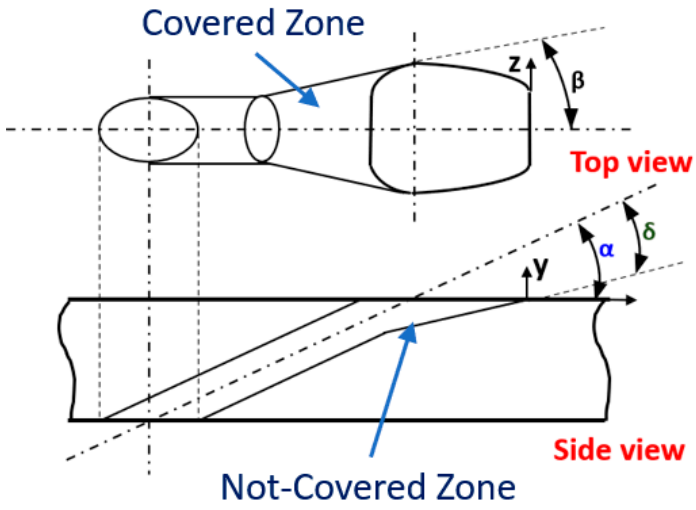

Figure 7. The concept of the film hole hood, the covered part of the expansion region, was alluded to by some authors, e.g., [35], but this parameter is mostly neglected in the literature [22,36].

Bunker [30], Bogard and Thole [37], and Han and Ekkad [38] provided a comprehensive review of the performance of shaped holes with diffused exits. Some common hole shapes in the film cooling literature are shown in Figure 4 [32]. A compilation of design data for turbine-related film cooling are available in the book *Gas Turbine Heat Transfer and Cooling Technology* [20]. LES simulation on different holes shapes was reported by Dupuy et al. [39], who noted that inhomogeneous turbulent boundary condition improves the prediction of film cooling. This LES-based observation is important and signified the need for design optimizations at the inlet of the film holes.

Gritsch et al. [40] investigated the adiabatic effectiveness of fan-shaped and laid-back fan-shaped holes with angle of inclination of 30° to the test surface for blowing ratio ($M = \rho_c u_c / \rho_\infty u_\infty$) up to 2. The lateral expansion at the exit in both the shaped holes was 14° and forward expansion of laid-back fan-shaped hole 15°. Local effectiveness contours obtained through 2D imaging for the investigated shaped holes and baseline cylindrical holes are shown in Figure 8 at three blowing ratios. Contrarily to the shaped holes, the cylindrical jet detached from the surface at the highest blowing ratio and provided relatively weaker lateral coverage of the coolant fluid. Amongst the shaped holes, fan-

shaped had higher centerline effectiveness, whereas laid-back fan-shaped had better spread downstream. In addition to the hole shapes, the curvature of the base surface can have a significant influence on the film characteristics [41]. The concave surface (pressure side of airfoil) tends to have inferior film performance than a convex surface. In real engine design, sometimes the pressure side holes are left round (not shaped) because the performance does not improve much with hole shapes. Inner flow structures of film injection have been discussed by Walters and Leylek [42] and Hyams and Leylek [36].

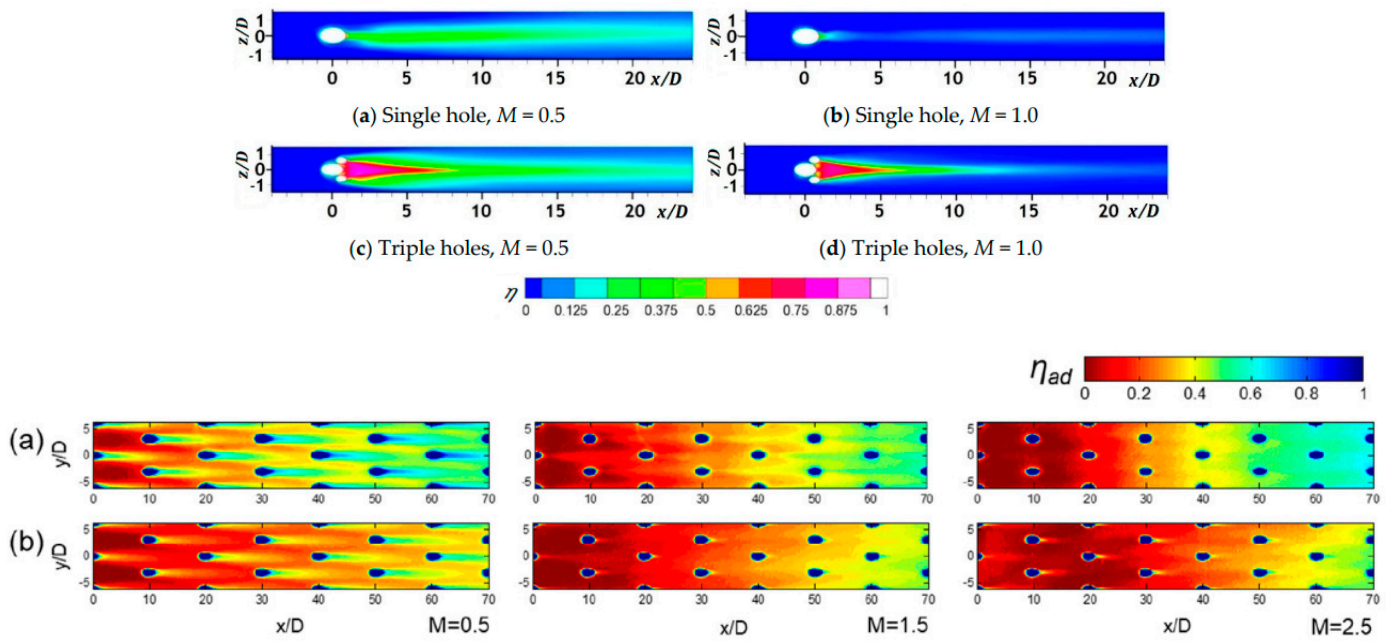

Figure 8. Local effectiveness η distribution for single and triple holes at different blowing ratios (0.5 and 1.0) [43]. Effect of blowing ratio on hole arrays are from Li et al. [44]. More on shaped hole effects were discussed in [40].

Kohli and Bogard [45] analyzed round, fan-shaped, and laid-back fan-shaped holes, but used a wider inclination of jet exit angle relative to the test surface (55° instead of 35°). Their investigation reported superior performance of the larger angle injection in comparison to standard 35° round hole. The angle of injection of the jet axis with respect to the test surface in industrial applications is typically around 30° to 40° [46]. Note that this angle limitation is imposed by the manufacturing techniques, and it is expected that favorable angles will be implemented by the adoption of additive manufacturing techniques. Details of near hole heat transfer coefficient were measured by Gritsch et al. [47]. They found that laidback fan-shaped holes provided a better lateral spreading of the injected coolant than the fan-shaped film hole, which led to lower laterally averaged heat transfer coefficients.

In film cooling, the holes can be inclined at an angle to the mainstream flow direction as well as being inclined to the test surface, and this angle is commonly referred to as the compound angle. Ligrani et al. [48] and Sen et al. [46] investigated film cooling holes with compound angles. Sen et al. [46] investigated round and 15° forward expanded holes with 60° compound angle as shown in Figure 9 at blowing ratios (M) varying between 0.5 and 2.5 and momentum flux ratio ($I = \rho_c u_c^2 / \rho_\infty u_\infty^2$) between 0.16 to 3.9. The flow structure of film showed interactions of counterrotating vortex pairs [49], and that was attributed to improved jet attachment to the surface.

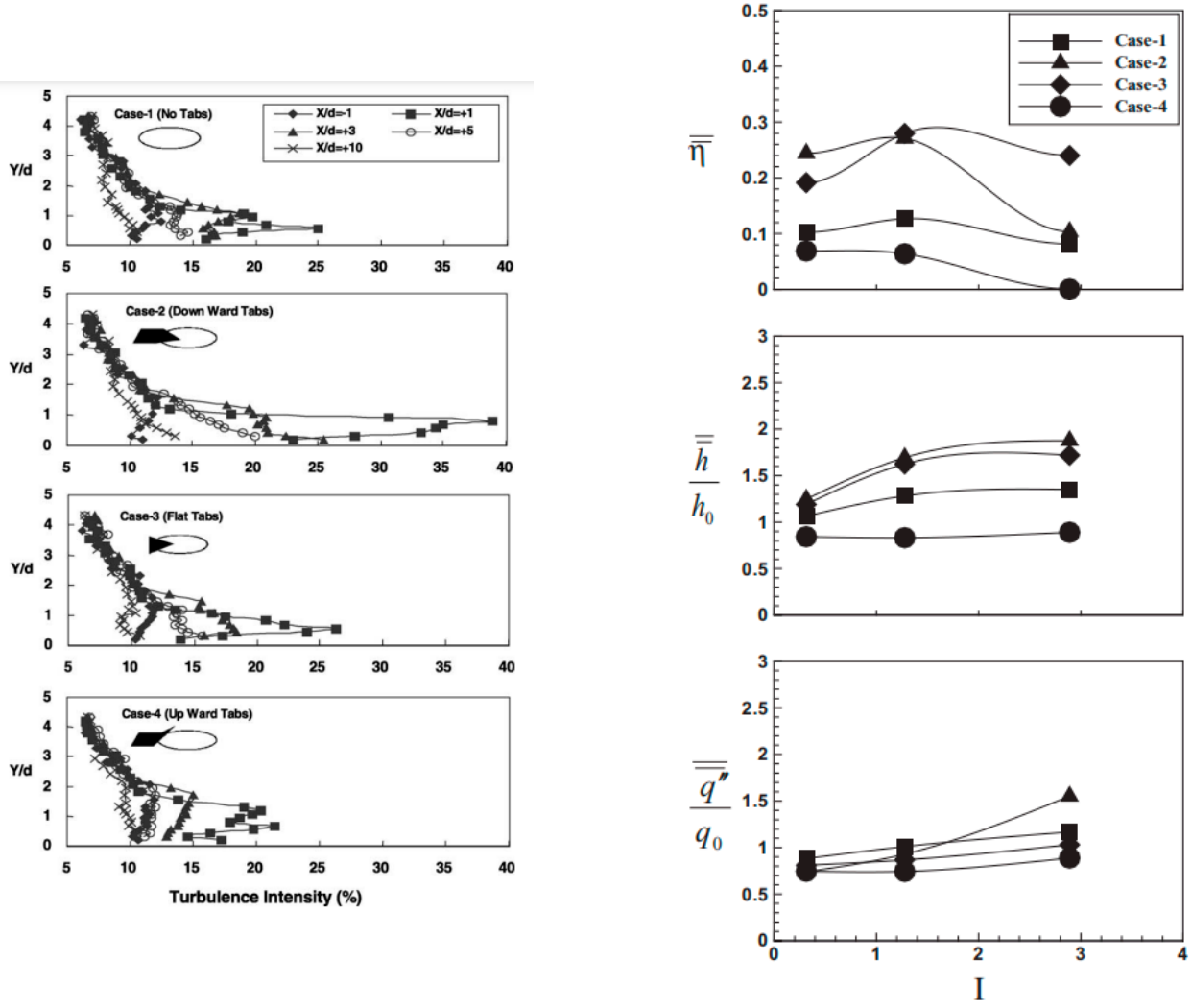

Figure 9. Film cooling with tabs and the effect of momentum flux ratio (I) were presented by Nasir et al. [50]. Heat transfer coefficient and net heat flux reduction trends for the compound holes at different momentum flux ratios were presented by [46].

Sen et al. [46] reported the mean adiabatic effectiveness and heat transfer coefficient distribution for the investigated shapes, where the compound-angled holes had higher adiabatic effectiveness with respect to standard zero compound angle configuration. Those plots could not be included here due to permission restrictions. The compound holes also yielded significantly higher heat transfer coefficients due to increased turbulence levels near the wall because of coolant-jet and mainstream flow interaction. Momentum flux is the dynamic head that signifies the aggression with which a coolant jet penetrates the mainstream flow and mixes with it; therefore, significantly higher heat transfer was observed at higher momentum flux ratios. For the forward-expanded 60° compound hole, maximum effectiveness was obtained at $I = 1$, but those flow conditions also yielded the maximum heat transfer coefficient ratio (h/h_0), resulting in overall net heat flux reduction value less than that incurred by compound round holes at $I = 0.25$. Nasir et al. [51] investigated a row of round holes with 0° and 60° compound angle to the flow and 55° inclination to the test surface for $M = 0.5$, 1.0, and 1.5, where higher adiabatic effectiveness and heat transfer coefficient was observed for compound holes. These investigations warrant the necessity of quantifying both the adiabatic wall effectiveness and heat transfer coefficient to measure the overall potential of the film cooling configurations as ranking the configurations based on their adiabatic film cooling effectiveness alone can be misleading. Figure 9 shows the

effect of placing a tab at the film hole exit. A properly designed tab showed to preserve the film cooling effectiveness for a larger distance than the configuration without a table. The trend in film effectiveness can be complex, as shown by Barigozzi et al. [28] in Figure 10. The film holes manufactured in conventional machining processes have to have the line of sight for the machine to drill holes, and that can be restrictive on deciding where the hole can be placed. AM removes that design restriction.

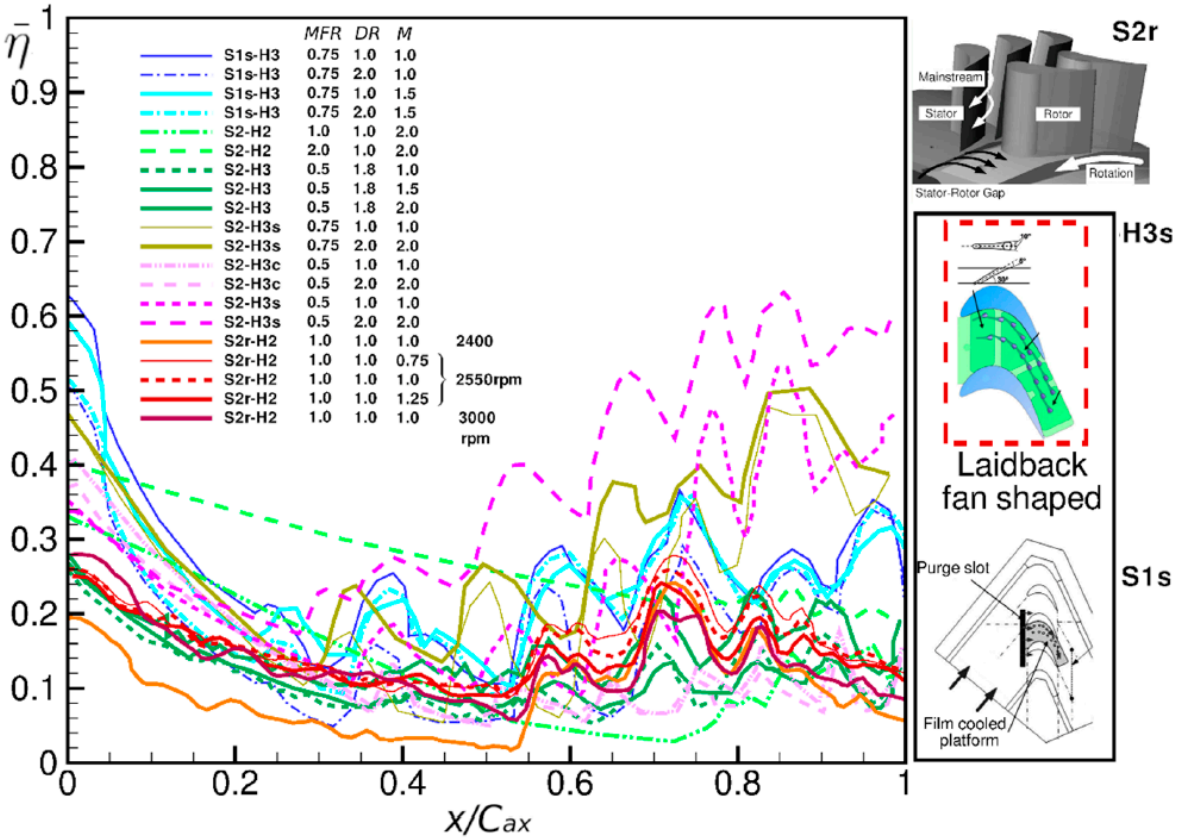

Figure 10. Film effectiveness curves can be complex and can have downward and upward trends [28] (courtesy: MDPI open source).

Schroeder and Thole [52] reported that about 130 different hole designs exist in the literature, but suggested the lack of a baseline configuration with which the performance of the novel shapes can be satisfactorily compared. Therefore, the authors proposed a 7-7-7 laid-back fan shaped hole that had circular metering section with diffused outlet having 7° expansion angle in each direction. The configuration parameters were selected based on the dimensional ranges reported in film cooling literature with an argument that the proposed design would demonstrate no in-hole jet separation. Unfortunately, they did not pay much attention to the hooded length.

Ekkad and associates [53–55] proposed novel antivortex turbine film cooling designs that had a tripod like arrangement with two secondary holes on either sides of the primary middle one. The design of anti-vortex holes was conceived to mitigate the effect of counter-rotating vortex pairs (known as kidney pairs) generated by the main hole to prevent the liftoff of the coolant by reducing the momentum flux from the main holes. The film cooling effectiveness and heat transfer ratios for different parametric values of the design have been analyzed and reported by the group. These anti-vortex holes could provide better film cooling effectiveness than standard cylindrical and diffused-exit holes at about 50% less coolant consumption.

Several studies mentioned above were conducted on holes flushed on a flat test plate because of the convenience in conducting experiments. Variations in the number of holes

or arrays have been explored in details by Ligrani et al. [48] They investigated single- and double-staggered rows of compound round holes for blowing ratios M = 0.5, 1.0, 1.5, and 1.74. Spanwise-averaged film cooling effectiveness for two row staggered compound holes was the highest at $M = 0.5$ and this effectiveness decreased with increasing M for streamwise distance of x/D < 20. Injectant liftoff was reported to be influenced by the momentum flux ratio, whereas the blowing ratio was significant in determining the coolant coverage characteristics. Figure 11 illustrates the effect of conductivity of the solid on full-coverage film effectiveness.

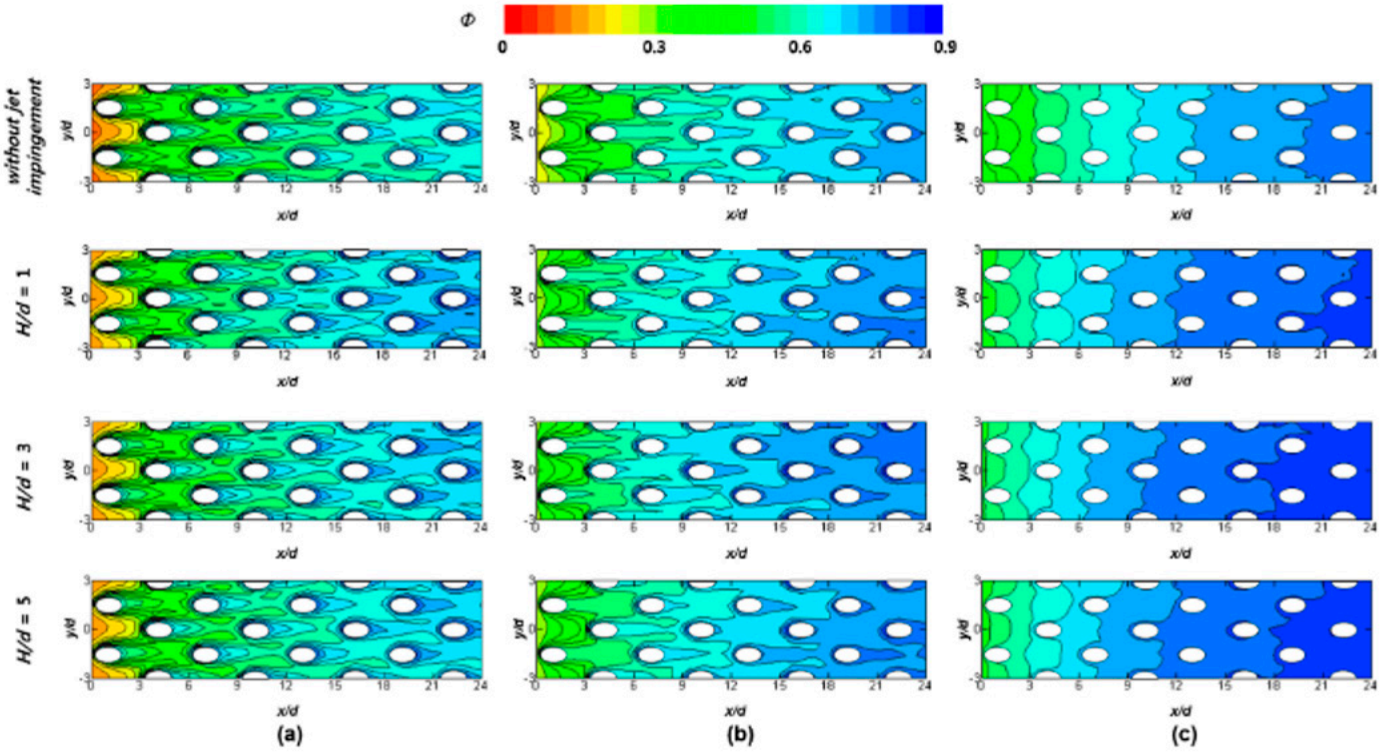

Figure 11. Total cooling effectiveness in a full-coverage film cooling with changing conductivity of the base plate in a flat plate configuration [56]. Thermal conductivities were (**a**) 0.2, (**b**) 1, and (**c**) 13.4 W/mK. As the conductivity increases, film streaks get blurred.

Multiple rows with full array film cooling over the entire flat test surface was investigated by Ligrani et al. [57] and Metzger et al. [58]. Combustor cooling employs such densely arranged film cooling holes. Ligrani et al. [57] investigated full-coverage film cooling with streamwise (6D and 18D) and spanwise (3D, 5D, and 7D) pitch values as the variables. For streamwise spacing of 6D, minimal increase in effectiveness was observed with increment in the blowing ratio (M) from 2 to 5 and no effect was present for $M > 5$. At fixed blowing ratio, effectiveness for dense array of streamwise distance of 6D was higher than sparse configuration having streamwise distance of 18D. Denser configuration with streamwise distance of 6D exhibited higher line-averaged values of heat transfer coefficient and net heat flux reduction.

Ekkad et al. [59] reported detailed film effectiveness and adiabatic film cooling effectiveness for two rows of holes oriented at $\pm 15^\circ$ from the stagnation line of a cylinder representative of the blade leading edge. Turbine blade leading edge experiences high heat flux and aerodynamic loads due to fluid stagnation. Therefore, film cooling in this zone is typically provided through an array of holes called showerhead. In a different study, Lu et al. [60] investigated the influence of angle and shape of holes in rows adjacent to the middle stagnation-line row in showerhead cooling through semicylindrical leading edge mounted on a flat after-body test model. Inclinations of the holes were 0°, 30°, and 45° to the test surface in the transverse direction. The study showed that the addition of

a third compound angle (inclination to test surface in spanwise direction) to the configurations increased the film effectiveness at lower blowing ratios without impacting heat transfer coefficient.

Ramesh et al. [61] reported film effectiveness results on the pressure and suction sides of the airfoil shapes. Similarly, several investigations by Han and group [62–64] in the post-2000 era were conducted on the real blade-like configurations. Gao et al. [63] performed experimental measurements on a test blade in a linear cascade of five-blade facility equipped with four rows of laidback fan-shaped holes on the pressure side and two rows on the suction side. Film cooling effectiveness decayed faster on the pressure side in comparison to the suction side due to jet liftoff. Better cooling performance at lower blowing ratios was present immediate in downstream regions of the holes but wider film coverage was obtained in far downstream regions at high blowing ratios as the coolant was convected back to the blade surface. The upstream wakes were artificially simulated with wake rods upstream of the cascade inlet and were found to have detrimental effect on the film coverage, especially in the mid-span region of suction side. Narzary et al. [65] analyzed the effect of coolant blowing ratio, coolant-to-mainstream fluid density ratio, and freestream turbulence on the adiabatic film effectiveness of a blade in a high pressure five-blade linear cascade facility. Two, four, and three rows of cylindrical holes were present on the suction side, pressure side, and around the leading edge of the test blade. An increase in the blowing ratio from 1.2 to 1.7 lead to significant improvement on the pressure side and enhancement of blowing ratio from 1.1 to 1.4 led to moderate augmentation in the effectiveness on the suction side. Augmentation in the freestream turbulence resulted in deterioration of effectiveness on pressure side but showed improved cooling performance at downstream distance beyond 0.45 axial chord length on the suction side.

The academic studies mostly focus on the near-hole effectiveness, but the turbine designers are more interested in the far-field effects such as distance of about 20–100 times of cooling hole diameter downstream of the hole exit. Unfortunately, most published work does not provide that data. Near-hole high effectiveness is not practically useful because the convection cooling in the hole can easily take care of the near hole region. Heat pickup in the film hole and the balancing effect on film can be optimized in a scientific way as discussed by Dutta and Smith [66,67].

2.2. Fluid Ratios

2.2.1. Density Ratio

Typical coolant-to-mainstream fluid density ratio (ρ_c/ρ_∞) in actual turbine applications is maintained around 2 to maintain a cooler (hence, heavier) film with respect to the incoming hot gases. Goldstein et al. [29] analyzed the effect of density ratio on film cooling performance of cylindrical and diffused-exit holes and found that the relatively denser fluid provided higher film cooling effectiveness at larger blowing ratios. Momentum flux ratio was identified as the key parameter in determining the penetrating capability of coolant jets of different densities into the mainstream flow. Pederson et al. [68] investigated the influence of density ratio ($\rho_c/\rho_\infty = 0.75$ and 4.17) for cylindrical holes inclined at 35° to the mainstream direction. Sinha et al. [69] investigated a row of cylindrical holes for a wide range of density ratios (ρ_c/ρ_∞ = 1.2 to 2.0) for their effect on the centerline effectiveness at blowing ratio of M~0.25 to 1.0 and momentum flux ratio varying between 0.05 and 0.83. Figure 12 shows the centerline effectiveness at different density ratios. Higher DR showed better film effectiveness. Sinha et al. [69] studied the effect of DR with different blowing ratios like M~0.5 and 1.0. The jet remained attached for M~0.5 showing a monotonic decrease with respect to the streamwise distance and the performance at both density ratios was similar. However, for higher mass flux, M~1.0, jet-detachment at the hole exit was apparent and the magnitudes of performance was significantly different as well. For higher density ratios (ρ_c/ρ_∞ = 1.6 and 2.0), the laterally averaged effectiveness showed maxima near the hole followed by monotonic decrease downstream of the hole at lower blowing ratios but as the blowing ratio increased, the jet exhibited minima near the hole exit

followed by continuous rise in value downstream. Increasing the density ratios generally increase the lateral average effectiveness at higher blowing ratios due to better spreading over the surface.

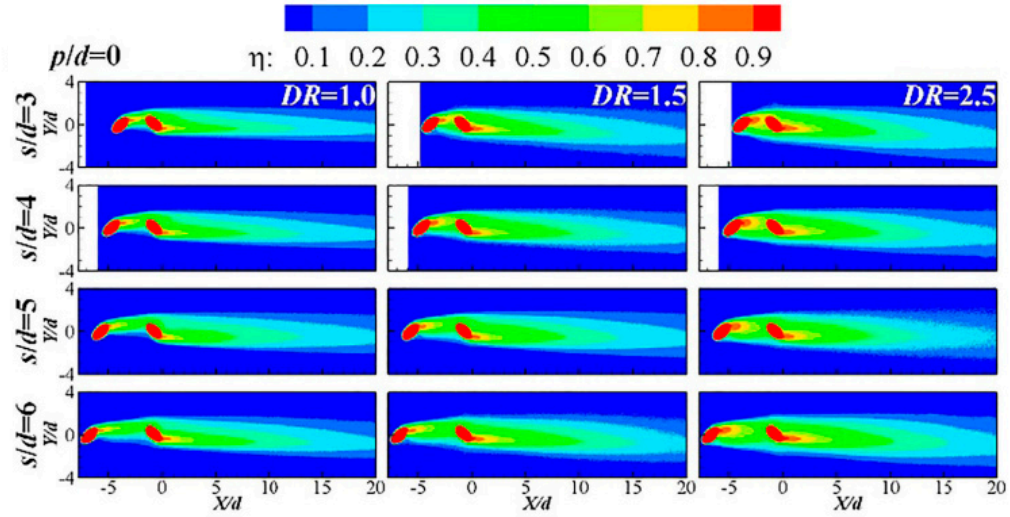

Figure 12. Inclined holes in tandem and the effect of density ratio were shown by Yao et al. [70]. Centerline effectiveness at different blowing ratios and density ratios were presented by [69].

Ekkad et al. [71] analyzed the effect of density ratios using air and CO_2 as injection coolant in an array of compound holes aligned at 45° and 90° to the mainstream flow using high resolution transient liquid crystal method. For both the coolants, higher effectiveness was provided by compound angle holes at the same blowing ratio. CO_2 provided lower heat flux ratio (q /q_0) than air at higher momentum flux ratios. More recently, Johnson et al. [72] used particle image velocimetry (PIV) and mass-transfer experimental techniques to quantify the flow and thermal processes in a row of cylindrical holes with 30° angle of injection for two different density ratios ρ_c/ρ_∞—0.97 and 1.5. The PIV analysis revealed that at blowing ratio of ~1.7, the coolant jet with lower density lifted off the surface, whereas the heavier coolant was still attached to the surface, yielding better film cooling coverage. The thermal analysis also showed the presence of finite effectiveness area upstream of the injection holes possibly due to entrainment of the coolant jet by the horseshoe-vortex. The density ratio effect results are consistent within the literature and align with the discussion presented above. Several other researchers have analyzed this variable, but not all of them are presented here for brevity. Readers are referred to a review provided by Ekkad and Han [73] for further details.

2.2.2. Blowing Ratio (M) and Momentum Flux Ratio (I)

Effect of blowing ratio (M), momentum flux ratio (I), and free-stream turbulence parameters on the film cooling performance has been reported by several researchers [46,74,75] in the last five decades. Some prominent studies and results are discussed herein to have a basic understanding of the general impact of these flow variables. Blowing ratio or mass flux ratio between 0.5 and 1.0 has been considered an optimum working range for the cylindrical holes beyond which jet detachment becomes profound and film cooling diminishes. Eriksen and Goldstein [76] analyzed an array of 35° inclined cylindrical holes with spanwise spacing of three diameters and found that heat transfer coefficient at low blowing rates were not much different from no-blowing case. The heat transfer enhanced with increasing M and at M~2, an increment of 27% in lateral average heat transfer was observed with respect to the no-blowing case. Peak heat transfer was generally located at the edges of the jets between the span of two adjacent holes due to enhanced turbulence.

Sen et al. [46] investigated heat transfer for an array of 35° cylindrical holes with 60° compound angle for M = 0.4 to 2.0 and I = 0.16 to 3.9, where the authors found that

large compound angles do not provide significant enhancement in heat transfer levels at lower values of momentum flux ratio. Several studies as listed here have investigated suitable scaling parameters at which the performance data measurements can collapse. Finding suitable scale allows one to directly compare the film cooling performance of configuration under investigation to another study by matching the scaling parameter. For cylindrical hole configurations, Sinha et al. [69] suggested that for attached jet (one that is not yet lifted off) centerline effectiveness scaled with mass flux ratio (M) and for detached-reattached jets at higher blowing ratios, effectiveness scaled with the momentum flux ratio (I). Decrease in density and increase in momentum flux ratio reduced the spread of the film cooling resulting in lower laterally averaged effectiveness. The authors showed that jet detached from the surface at larger momentum flux ratios caused drop in the effectiveness. Later, Schroeder and Thole [52] showed that the effectiveness of the shaped holes did not scale with mass flux or momentum flux ratios for $M > 2$ at density ratios of 1.2 and 1.5. Ammari et al. [77] analyzed heat transfer values on a flat plate rendered by hole with 90° (normal) and 35° injection angle to the test surface. Density ratios of ρ_c/ρ_∞ ~1.0, 1.38 and 1.52 were investigated with blowing rate of M ~0.5–2.0. Heat transfer data of normal injection hole scaled well with the mass flux ratio, whereas 35°-hole data collapsed better for velocity ratio (u_c/u_∞) at any fixed streamwise distance x/D.

Determination of a parameter to scale the laboratory-obtained results to the engine-relevant conditions is important and mixed success has been achieved on this issue. Density ratio achieved in real operating conditions is around 2, therefore, making it an important non-dimensional parameter to be scaled or replicated. Several parameters such as blowing ratio, momentum flux ratio, or velocity ratio have been considered in prior investigations to scale film cooling effectiveness across varying density ratios as discussed above, but the consistent trends were not observed. In case an appropriate parameter is found to scale the effectiveness across wide density ratio range, it would help in circumventing the need to match density ratios in experiments.

Film effectiveness with varying momentum flux ratio and density ratio was illustrated by Li et al. [78]. The momentum flux ratio on a film cooled turbine platform is shown in Figure 13.

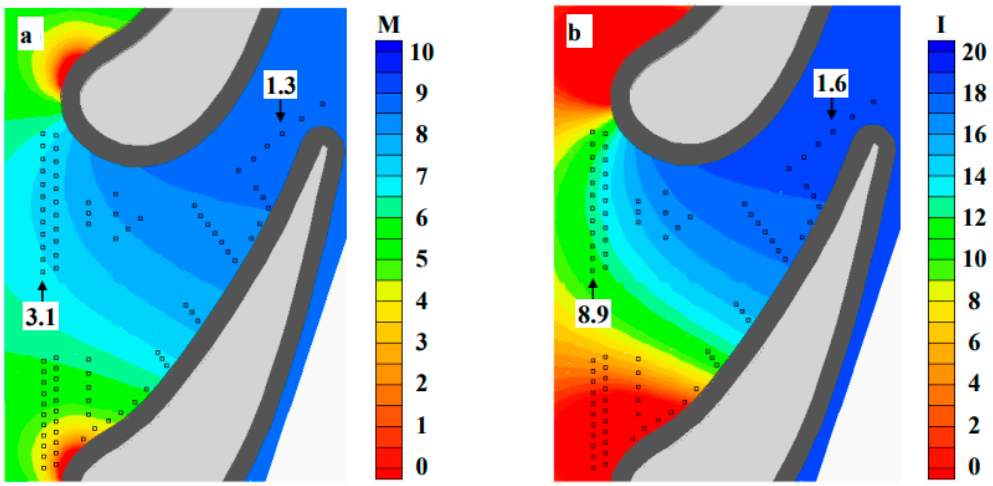

Figure 13. Blowing ratio and momentum flux ratios can be different for the same film configuration as shown by [79]. Film effectiveness comparison of low and high momentum flux ratio (I) and comparative effect by density ratios (DR) were shown by [78,80].

2.3. Advective Capacity Ratio (ACR)

Quite recently, a new scaling parameter called advective capacity ratio (ACR = $c_{P,c}\rho_c u_c / c_{p,\infty}\rho_\infty u_\infty$) has been advocated by several authors [81,82] with the argument that considering the temperature differences, it is not only the density but the specific heat capacities of the fluids that influence the distribution of effectiveness. Rutledge and Polanka [82] numerically investigated the influence of Reynolds number ratio, Prandtl number ratio, and ACR on the adiabatic effectiveness and heat transfer coefficient of a single cooling hole. Density ratio demonstrated the most dominating effect; however, thermal conductivity and heat capacity variations also resulted in about $\geq$10% higher deviation in heat flux when scaled to engine-relevant conditions. Even matching both the blowing ratio and momentum flux ratio resulted in underprediction of effectiveness and heat transfer coefficient. Fischer et al. [81] performed experiments on a 7-7-7 shaped hole embedded in a flat plate and reported that ACR could exactly scale the adiabatic effectiveness while the jet remained attached, i.e., $I < 0.5$ in their study. The authors emphasized that as long as ACR is matched in experiments, there is no need to have matching density ratio, however, this is found to be true only for low momentum flux ratios. This ACR parameter is promising and can be explored further for various types of hole geometries and operating conditions to establish its robustness and fidelity in scaling the film cooling performance.

2.4. Freestream Turbulence

Schmidt and Bogard [80] reported the effect of freestream turbulence on the film cooling effectiveness of cylindrical holes inclined at 30° to the test surface at mass flux ratio of M = 0.6, 1.0, and 2.0, and the corresponding momentum flux of I = 0.18, 0.5, and 2.0. For $0.1 < I < 0.5$, high freestream turbulence reduced the peak laterally averaged effectiveness by ~50% as compared to that at low turbulence level conditions. However, interestingly the trend reversed for $I > 1$, where laterally averaged effectiveness at higher mainstream turbulence was superior. The increment in effectiveness at higher free-stream turbulence was attributed to the capability of turbulent mainstream flow to disperse the coolant better over the surface and push it back towards the surface wall after it lifts off at higher momentum flux values.

Saumweber and Schulz [83] investigated the cylindrical and fan-shaped holes, both with inclination of 30° with respect to the test surface, at fixed density ratio of 1.75 and varying turbulence intensity (Tu ~2.0% to 7.5%). The authors emphasized that the performance enhancement of shaped holes with respect to cylindrical holes at the low turbulence levels maintained in laboratory conditions was overestimated. Larger free-stream turbulence intensity was more detrimental for the shaped holes than for the cylindrical holes. Ekkad et al. [59] studied the effect of freestream turbulence and coolant density on the two rows of injection holes located ±15° from stagnation line of cylindrical test model. Air provided highest effectiveness at blowing ratio M = 0.4 whereas CO_2 provided the peak effectiveness at M = 0.8. The high-resolution data obtained through transient liquid crystal thermography showed that regions of higher effectiveness did not coincide with higher heat transfer zones. Increment in freestream turbulence had weak impact on the Nusselt number values of both investigated coolants, but the film effectiveness was significantly influenced at lower blowing ratios.

3. Measurement Techniques

The adiabatic surface temperature measurements in earlier investigations were performed by mounting finite number of thermocouples at discrete locations on test plates. The spatial trendlines were generated from this discrete data and the distribution of the effectiveness and heat transfer coefficient on the surface was interpreted. Achieving fully adiabatic wall conditions and eliminating conduction errors in these experiments was challenging due to which mass-transfer experiments gained attention. If the Lewis number (ratio of thermal diffusivity to mass diffusivity) is maintained nearly unity, then the mass transfer analogy can be used to find temperature on an impermeable wall. Goldstein [6]

pointed out that both the turbulent and molecular Lewis number should be around 1 to validate the analogy between mass and heat transfer. This can be achieved in highly turbulent flows where the turbulent Lewis number can be safely assumed to be around unity. Departure of molecular Lewis number from unity in highly turbulent flows might not be consequential for the final performance; however, maintaining turbulent Lewis number around unity is of prime importance. Han and Rallabandi [84] emphasized that while the flow is turbulent over most of the surface of turbine blades due to high Reynolds number assisted by turbulence enhancing secondary mechanisms involving vortices, coolant jets' penetration into mainstream flow, and wake formations, the flow in the vicinity of the leading edge could still be either laminar or in transitional stage, thus invalidating the analogy in this region. Despite these limitations, mass transfer techniques are still used because of their benefits over thermal methods. Mass transfer methods such as naphthalene sublimation technique has been used by Goldstein and Jin [85] to quantify film cooling effectiveness; however, naphthalene was found to have serious health-related issues and its use was discontinued. The mass transfer technique used in recent investigations are usually pressure sensitive paints (PSPs).

Development of fast thermal methods such as transient liquid crystal (TLC) thermography and infrared imaging (IR) also provided an opportunity to obtain temporal and high-resolution spatial variation of effectiveness and heat transfer coefficient contours. These methods have been widely accepted in turbomachinery community, and a brief description of these is provided below.

3.1. Transient Liquid Crystal (TLC)

This technique commonly employs one-dimensional semi-infinite heat conduction model with convective type boundary condition at the surface, which gives the final solution for temperature as following [50,55,86]:

$$T_w - T_i = \left[1 - exp\left(\frac{h^2 \alpha t}{k^2}\right) erfc\left(\frac{h\sqrt{\alpha t}}{k}\right)\right](\eta T_c + (1-\eta)T_m - T_i) \quad (4)$$

where T_i is the initial test surface, T_m is the mainstream temperature and T_w is the wall color change temperature. Two similar transient runs are conducted to obtain two equations, which can be then simultaneously solved to obtain η and h. For example, Nasir et al. [50] performed first run with mainstream heated to 58 °C and the coolant heated slightly above room temperature. In the second run, the coolant was heated slightly above mainstream temperature. Several factors such as lighting, calibration test, and conduction errors in the zones of high thermal gradients immediately near the hole exits affect the results. The final solution needs to be corrected for the conduction errors in the vicinity of holes.

3.2. Transient Infrared Imaging (IR) and Temperature-Sensitive Paint (TSP)

Ekkad et al. [87] were the first ones to use transient IR technique to capture the film cooling performance, where both the adiabatic film effectiveness and heat transfer coefficient were evaluated from a single test run based on the methodology proposed by Vedula and Metzger [88]. The solution of the temperature is similar to the one-dimensional conduction equation provided in Equation (4), but in this IR method, the temperatures are recorded at two instances of time (t_1 and t_2) in the same run:

$$\frac{T_{w1} - T_i}{T_f - T_i} = \left[1 - exp\left(\frac{h^2 \alpha t_1}{k^2}\right) erfc\left(\frac{h\sqrt{\alpha t_1}}{k}\right)\right] \quad (5)$$

$$\frac{T_{w2} - T_i}{T_f - T_i} = \left[1 - exp\left(\frac{h^2 \alpha t_2}{k^2}\right) erfc\left(\frac{h\sqrt{\alpha t_2}}{k}\right)\right] \quad (6)$$

The above two equations obtained from same transient run can be solved to obtain η and h. The advantage of this technique over the above discussed TLC method is that it requires only one test run to determine variables of interest, and there is no limitation of operating temperature band as imposed by the use of liquid crystals in TLC method. Also, transient IR method allows one to capture the initial temperature distribution on the surface. IR is used for surface temperature measurement, but the optics requires that viewing window is IR transparent. An alternative temperature measurement is TSP (temperature-sensitive paint) that can be viewed without any specialized window material. A fast measurement technique with TSP is illustrated by Bitter et al. [89] in subsonic flows.

3.3. Pressure-Sensitive Paints (PSP)

Pressure-sensitive paints use mass transfer technique, which eliminates conduction-related errors that inherently occur in thermal methods. Pressure-sensitive paints (PSP) are composed of luminescent molecules that are suspended in a polymer binder to form a paint. When these luminescent molecules are excited by blue light with wavelength around 400 nm, the excited particles have two routes to get back to the ground state. One is to emit light at longer wavelength (greater than 600 nm in red spectrum) and the second route is to interact with surrounding oxygen molecules (known as oxygen quenching) in which case the fall back to lower energy state does not emit light radiation. Therefore, the intensity of emitted red light can become function of the oxygen partial pressure adjacent to the PSP layer. A calibration test is conducted to find a relationship of the emitted intensity with that of the oxygen partial pressure, with an added caution that the calibration is performed at the same reference temperatures at which the actual tests have to be conducted. Introduction of a secondary gas through film cooling essentially modifies the oxygen concentration in vicinity of PSP and the corresponding light intensity is recorded. From the calibration test, the partial pressure corresponding to the recorded intensity values can be evaluated and further related to concentration and effectiveness, as follows (where $C_{O_2,C} = 0$):

$$\eta \approx \frac{C_w - C_\infty}{C_c - C_\infty} = \frac{C_{O_2,\,fg} - C_{O_2,air}}{C_{O_2,C} - C_{O_2,\,air}} = 1 - \frac{C_{O_2,\,fg}}{C_{O_2,air}} \tag{7}$$

With special cases such as nitrogen as foreign gas where the molecular weight is similar to that of air, Equation (7) becomes:

$$\eta \approx 1 - \frac{C_{O_2,\,fg}}{C_{O_2,air}} = 1 - \frac{P_{O_2,\,fg}}{P_{O_2,air}} \tag{8}$$

More details on this are available at Zhang and Jaiswal [90]. Han's group [84] at Texas A&M University have reported extensive film cooling research using the PSP technology in the last fifteen years. Wright et al. [91] compared the film cooling results obtained for seven equally spaced holes with injection angle of 30° and compound angle of 45° using three measurement techniques, viz. infrared thermography (IR), pressure-sensitive paint (PSP) and temperature-sensitive paint (TSP). The comparison showed that results of all these techniques were very different at lower blowing ratio M = 0.6, where the differences were amplified near the hole exit. The authors did not account for conduction errors in this region causing higher film effectiveness values with thermal methods like IR and TSP than that with PSP. At higher blowing ratios M = 1.2, the data downstream of the holes showed good match among the three techniques; however, the near-hole dip in film effectiveness due to jet detachment was not captured effectively by the IR- and TSP-based methods. Russin et al. [92] illustrated the TSP and PSP techniques on film cooling measurements. They used PSP for the film cooling effectiveness without the conduction effects and then used TSP to measure heat transfer coefficients in the presence of film cooling. Other notable publications with TSP include [63,93].

Gao and Han [94] used PSP technique to obtain film effectiveness characteristics from three- and seven-rows arrangement on a semi-cylindrical blunt body (that mimicked the

trailing edge) at blowing ratios M = 0.5 to 2.0 with radial and compound-angled holes. Seven-row design exhibited better cooling performance because of better film accumulation on the surface. The contours of film cooling effectiveness with PSP measurement are shown in Figure 14. Film cooling effectiveness distribution contours for seven-row design were obtained using PSP technique by Gao and Han [94]. Several other investigations on film cooling have been reported by Han and associates [95,96] with focus on the leading edge. Rallabandi et al. [97] analyzed the density ratio and unsteady wake effects (generated with vortex shedding from rods) on film cooling of turbine blade using PSP. Increasing the blowing ratio decreased film cooling on both suction and pressure side; however, at higher blowing ratios, the flow reattached on the pressure side due to concavity lending higher effectiveness downstream. Unsteady wakes shortened the film cooling traces without significant detrimental effect on the pressure side.

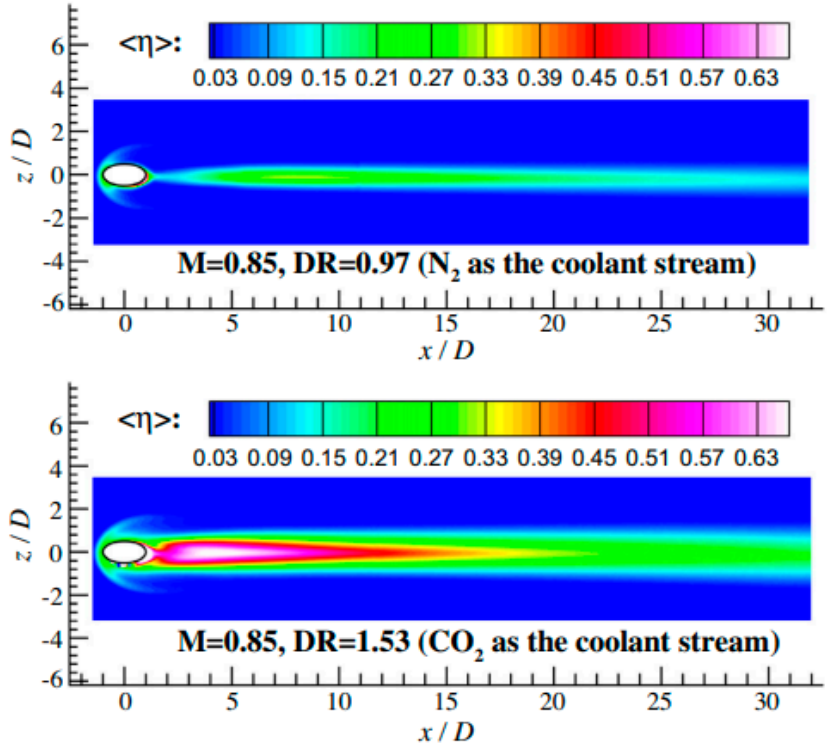

Figure 14. Film cooling effectiveness with PSP technique [72].

4. Curvature and Roughness

Even if most studies and measurements were conducted on flat surfaces, the airfoil is far from flat. Besides curvature of the wall, the flow accelerates or decelerates depending on the side of the airfoil, and it is well known that the blade passage fluid mechanics is very complex. Figure 15 shows the effect of curvature on film effectiveness without the complexities from end-wall effects. The pressure side clearly shows lower values than the convex suction side. As a result, there are usually more film holes in the pressure side than suction side. It has also been observed that using costly shaped holes in the pressure side does not add much benefit and thus many airfoils use simple round holes for the pressure side cooling.

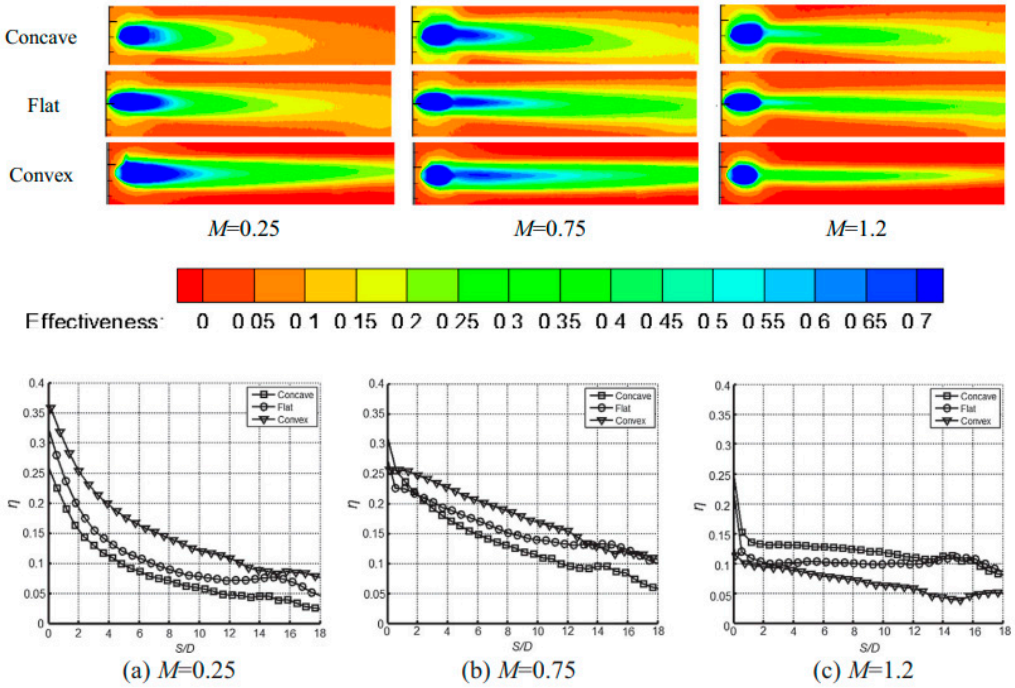

Figure 15. Effect of curvature on film effectiveness [98]. More on curvature effect concave surface (pressure side) and convex surface (Suction side) in Schwarz et al. [41].

Surface quality rendered by the adopted manufacturing technology plays significant role in determining the overall film cooling performance and a defining variable of this surface quality is the "roughness". The alternative additive manufacturing routes, especially laser powder bed fusion (LPBF)-based technologies, result in roughness scales that can significantly alter the film cooling performance. Therefore, it is imperative to have thorough understanding of the role that roughness plays in dictating the cooling characteristics in turbine blades. This section provides an account of prior reported investigations where the roughness of conventionally built blades was accounted for in discussing the film cooling performance. The following section will then discuss in detail the role of roughness rendered by additive manufacturing technologies in particular.

Bunker [99] highlighted that the EDM technology can provide uniform surface finish with roughness heights of about 2.5 µm whereas laser drilling yields relatively irregular hole diameter and inferior surface finish. Water-jet drilling can produce clean holes with shaped exits under controlled conditions. Marimuthu and Smith [100] reported the roughness of holes drilled via water-jet guided laser at an acute angle over thermal barrier coated nickel superalloy to be around 1.15 µm. Apart from the roughness incurred during manufacturing, the continued operation subjects the blade surfaces to deposits, pitting, erosion, and spallation, which generates roughness on the surfaces, as highlighted by Bons et al. [101]. Bons et al. [101] and Bogard et al. [102], targeted spatial nonuniformity in the roughness levels that persists on the surface of the blades. Figure 16 shows that film cooling effectiveness is susceptible to this spatially varying roughness near the injection and downstream.

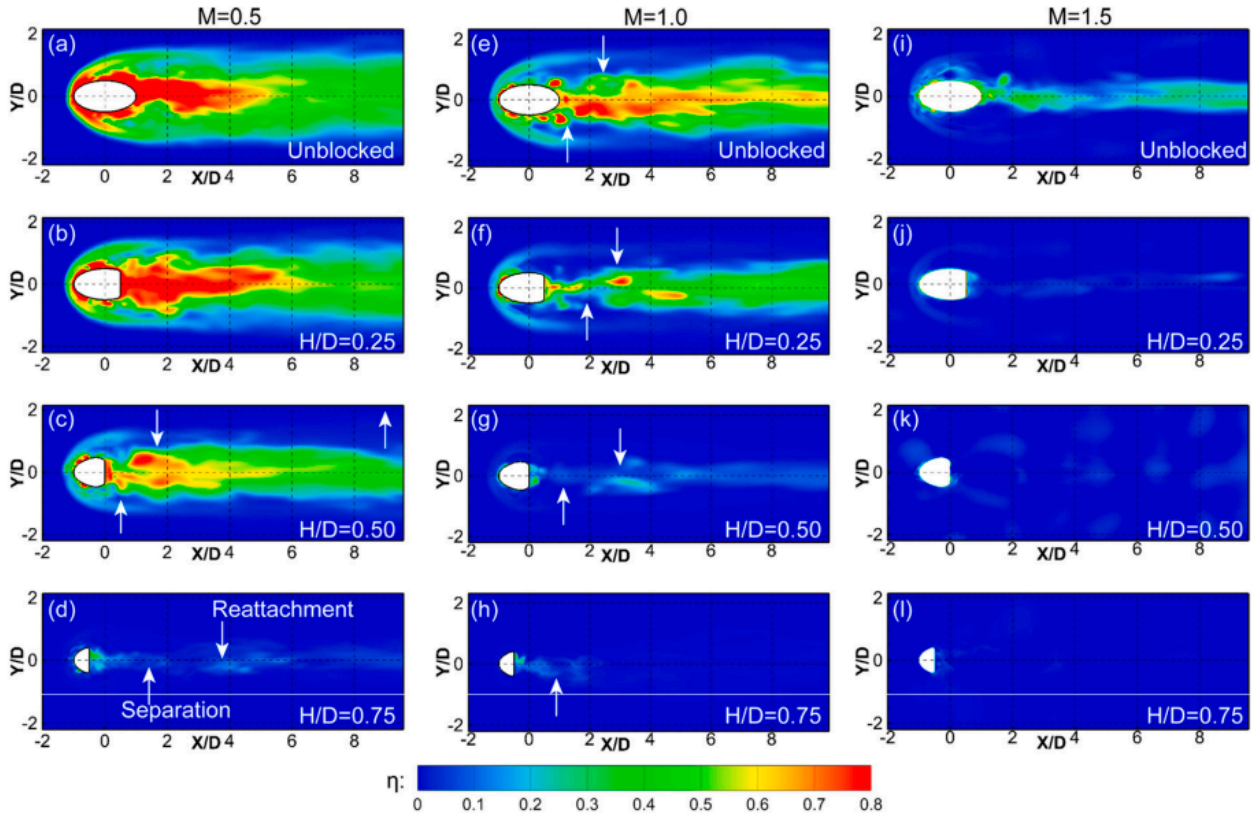

Figure 16. Film cooling effectiveness with different blockage levels [103] on flat surface. A reduction in film effectiveness happens with increased surface roughness [104]. The trend is captured in numerical simulations by Zamiri et al. [105].

Zamiri et al. [105] used LES to show that the film effectiveness reduces with increasing surface roughness. In another publication, Zamiri et al. [106] slightly overpredicted the film cooling effectiveness with LES in a smooth flat surface configuration, but the overall decay pattern was captured successfully. LES has significant potential to capture and characterize the inner details. A full paper on LES in turbine cooling is feasible because so many publications available on that topic. Due to lack of space and theme of this article, only a limited discussion on LES is provided as supporting evidence. Goldstein et al. [107] analyzed actual working turbine blade and found that the roughness was primarily present upstream of holes on the suction side and downstream of holes on the pressure side. Authors [107] then used cylindrical roughness elements in staggered type arrangement to study its impact on film cooling of one/two rows of cylindrical holes. At higher blowing ratios, 40–50% improvement in adiabatic wall effectiveness of single row of holes was observed due to enhanced turbulence and mixing with rough surface that dissipated the injected flow, preventing it from penetrating farther into mainstream flow. Although not quantified by the authors, the heat transfer coefficient values were also expected to be significantly increased over those with the smooth surface. Due to roughness-caused mixing, more spanwise uniformity in film cooling effectiveness occurred. Schmidt and Bogard [80] reported that at higher investigated turbulence level (~17%), laterally averaged effectiveness of rough surface modeled using conical elements was higher than the corresponding smooth configuration at blowing ratio of 0.6 because of the suppression of turbulent mixing. These past studies mimicked the roughness on the plane surface by using engineered roughness elements such as cylindrical and conical elements. While roughness upstream and downstream of the holes could be replicated conveniently with accessible surface modifications, the in-hole roughness replication is challenging.

Effect of in-hole roughness was investigated by Schroeder and Thole [104] on coupons of polystyrene in which a single array of 7-7-7 laidback fan-shaped holes was excavated using CNC milling machine with roughness varying between $Ra/D \sim 0.003$ and 0.020. These manufactured dimensions were well within the limit of 5% from the intended design. In comparison to smooth holes, the holes with higher roughness levels demonstrated a decrease of 60% in the area-averaged adiabatic effectiveness at the highest blowing ratio $M = 3$. Figures 17–19 show the AM design for turbine components. The normalized temperature contours on AM surface as well as on the y-z cross-plane located at $x/D = 4$ downstream of the holes were shown by Schroeder and Thole [104], at blowing ratio of 3. For smoother holes, the kidney-shaped profile was observed with better lateral coverage and lesser penetration into the mainstream as compared to rougher hole. In-hole roughness elements were considered responsible for creating narrow high-velocity jet core with thicker boundary layers along the interior walls of holes, which penetrated higher into mainstream flow. In-hole roughness was reported to be capable of reducing the film cooling effectiveness by >2 times at higher blowing ratios. The performance of the rougher holes was diminished relative to smooth holes at both lower (0.5%) and higher (13.2%) investigated turbulence levels.

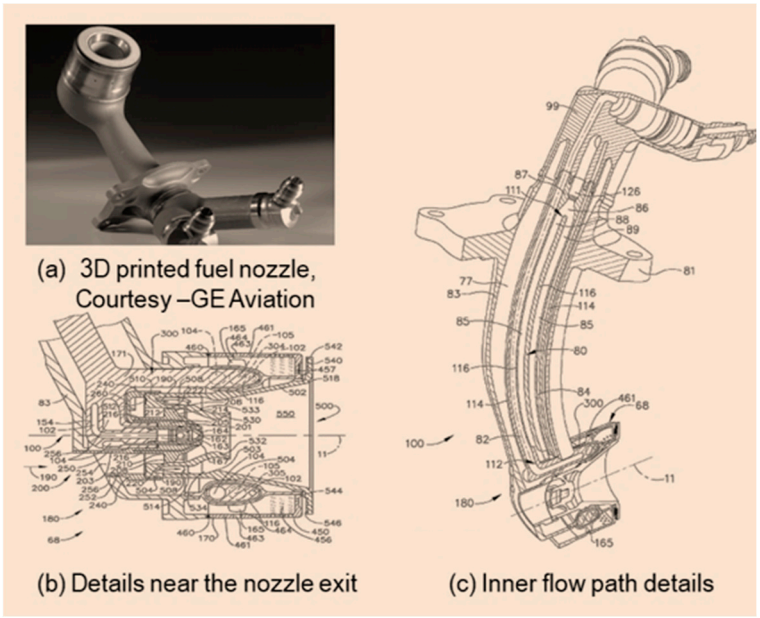

Figure 17. A successful implementation of AM in mass production is LEAP engine fuel nozzle (images [108,109]).

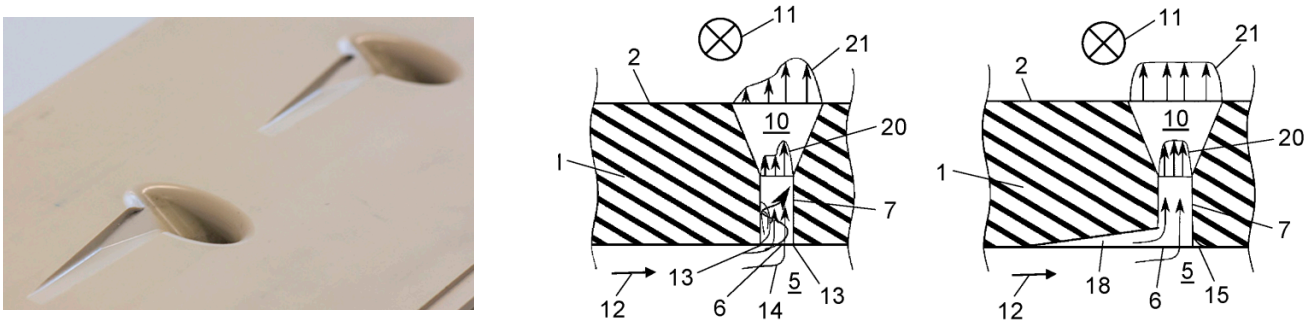

Figure 18. Aerodynamic film cooling hole inlets [110,111]. Rounded with NACA inlet to the film hole [112].

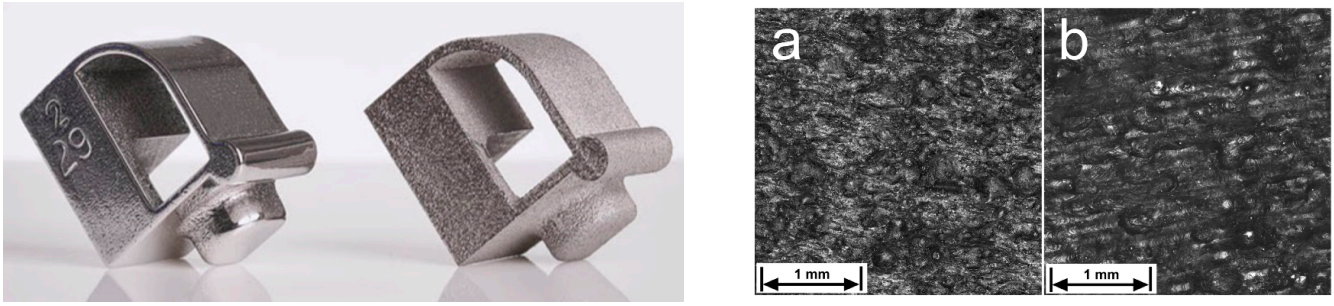

Figure 19. Surface finish before and after postprocessing of AM component (Fintek) [113]. Roughness on surface can be different based on build orientation [114].

5. Additive Manufacturing (AM)

Additive manufacturing has emerged as an alternative route to realize relatively sophisticated film cooling designs that are otherwise very difficult, if not impossible, to manufacture using conventional manufacturing technologies. Dutta et al. [115] discussed engineering and economic aspects of additive manufacturing in energy-related industries. The blades/holes made through conventional processes manifest low surface roughness after many machining hours; on the contrary, the roughness in AM route is inherently present during thermal printing, making it an important design variable along with the geometry and flow conditions discussed in the previous sections. Figure 17 shows the complex structures feasible with the additive manufacturing, and Figure 18 shows a new film hole design used for tilting the film to the more needed side coverage. One major contribution from AM can be alterations of the internal features. Conventional machining altered the visible parts of the film hole due to accessibility issues. AM can accommodate modifications to the inlet of the film hole to improve coolant distribution.

5.1. AM Surface Roughness

Figure 19 shows the actual scale AM surface roughness and that can vary with build orientation. Scanning electron microscope images of film cooling holes for actual scale AM coupon, actual scale EDM coupon, and 2 × scaled AM coupon were illustrated by Stimpson et al. [16]. Nondimensional temperature contours for smooth and rough holes as well as effectiveness, η, was measured on wall using IR camera; and thermal field θ measured on y-z plane located at x/D = 4 downstream of the hole exit using fine-wire thermocouple rake were performed by Schroeder and Thole [104]. Actual scale EDM hole, and 2 × actual scale AM holes were built with vertical and angled orientations. Metering section in the AM holes was rougher and more clogged in comparison to EDM hole. EDM hole demonstrated higher overall effectiveness values for the entire investigated range of blowing ratios where internal cooling Reynolds number (and hence the contribution of internal convection) was held constant at any investigated case. This is because of lower mass flow rate in the AM holes at the same internal-channel Reynolds number due to lower effective metering area, and also because in-hole roughness tended to provide jet liftoff tendency to the ejected fluid. In-hole convection with roughness becomes the dominating near-hole cooling contributor at higher blowing ratios.

Aghasi et al. [116] compared the film cooling performance of 7-7-7 shaped diffusing hole proposed by Schroeder and Thole [52] manufactured through three different AM technologies: fused deposition modeling (FDM), stereolithography (SLA), and polyjet (see Figure 20). The blowing ratio (M) was varied between 1 and 3.5 at mainstream Mach number of 0.30 and density ratio of 1.5. The designed hole diameter (D) was held constant at 0.1 inches, i.e., 4 to 5 times bigger than typical hole size of an actual high pressure turbine blade (0.020 in–0.024 in). The relative roughness (with respect to hole diameter) was the highest for FDM ($Ra/D \sim 0.01$) and the least roughness was observed for SLA ($Ra/D \sim 0.005$). The span-averaged film cooling effectiveness was higher for rougher

coupons at the highest M~3.5 because of the spread of coolant caused by the roughness and inhibition of the flow to strongly penetrate the mainstream flow. It should, however, be noted that through these technologies, the coupons were printed either in photopolymer or plastic material, whereas the practical applications used high-temperature alloys. The adiabatic film cooling effectiveness and heat transfer values obtained from smooth coupons can be fairly scaled to the actual operating conditions; however, such an exercise for additively manufactured samples should be conducted cautiously. That is because the roughness signature of additively manufactured polymeric/plastic material are going to be different from that present on the metal. Moreover, the influence of roughness with scaled up geometries can significantly deviate from that in actual smaller dimensions, for e.g., more profound obstruction can occur in holes printed with smaller metering diameters.

A numerical study by Shi et al. [117] showed the AM-related surface roughness decreased the cooling effectiveness. They also found unequal coolant distribution in the film holes caused by the surface roughness. Design optimization based on hole blockage due to manufacturing uncertainty was carried out by Lee et al. [118]. Manufacturing deviations and related uncertainties can be more problematic in supersonic condition [119]. Partial hole blockage could occur due to particle deposition or thermal barrier coating (TBC). Lee et al. [118] found that TBC-induced hole blockages had more detrimental effect on film cooling performance than the AM-induced in-hole and blade surface roughness.

Coupons made with laser powder bed fusion (LPBF) technology with internal channels capable of supplying coflow or counterflow movement of coolant with respect to mainstream flow was analyzed in a series of paper by Thole and group [16,120,121]. The common design and flow conditions in these investigations were as follows. The samples were printed in nickel alloy that is typically used in high-temperature applications. The coupons are shown in Figure 3a, and they were built with two major orientations, one with the vertical hole axis and other with the face of the coupon inclined at 45°. The holes were printed at the scales of actual turbine applications, and the experiments were typically conducted at Biot number and h_∞/h_i (mainstream to internal cooling channel heat transfer coefficient ratio) matching with those encountered in real engines. The results were therefore directly scalable to industrial operations. Since the entire test coupons were printed in metal, the conjugate cooling performance of the holes was given in the form of overall cooling effectiveness (ϕ):

$$\phi = \frac{T_w - T_\infty}{T_c - T_\infty} \tag{9}$$

Jung et al. [56] studied full-coverage film cooling with various Biot numbers. The cooling effectiveness was observed to be of the order of 87% at low Biot number cases. As the Biot number was decreased from 4.04 to 0.06, the cooling effectiveness increased by 23%.

In configuration with internal channels like that shown in Figure 3b, three major mechanisms of heat transfer determine the overall performance: external surface film cooling, inside film hole convection, and inner airfoil surface convection. Conjugate optimization of all three heat transfer mechanisms was explored by Dutta and Smith [122]. They showed that local hole diameter adjustment can result in lower thermal stresses due to more uniform metal temperatures. Stimpson et al. [16] showed that the build orientation could impact the overall effectiveness of the holes as the resulting surface roughness characteristics were different. Vertical orientation was found to be more favorable for the construction of laidback fan-shaped hole as it provided no profound hole blockage and lower roughness in comparison to angled orientation. For comparison of the surface quality, a separate solid (no holes) coupon was manufactured with AM in which holes were cut through EDM technology. Moreover, the scaled up versions of the additively manufactured coupons were also generated for testing and analyzing.

5.2. AM New Hole Shapes

Snyder et al. [121] additively manufactured six different hole-shapes, viz. 7-7-7, console, crescent, oscillator, and tripod. The microscopic images of the manufactured hole exits are shown in Figure 21. Metering area was oversized by about 20% from the designed real engine values. Console, crescent, and tripod provided better cooling coverage because of proximity of the hole exits. As seen in Figure 21, the thin features at the exits of the hole were distorted, which severely affected the uniformity of cooling on the surface. Stimpson et al. [120] analyzed the effect of coolant flow direction and found that the overall effectiveness of 7-7-7 holes was higher with coflow direction. It was found that increased roughness in the film cooling hole resulted in decreased effectiveness. Vinton et al. [123] investigated the full-array coverage film cooling coupons manufactured through direct metal laser sintering (DMLS) technique for blowing ratio range of 0.5 to 6. Presence of in-hole roughness diminished the laterally averaged film cooling effectiveness by 50% when compared with prior studies.

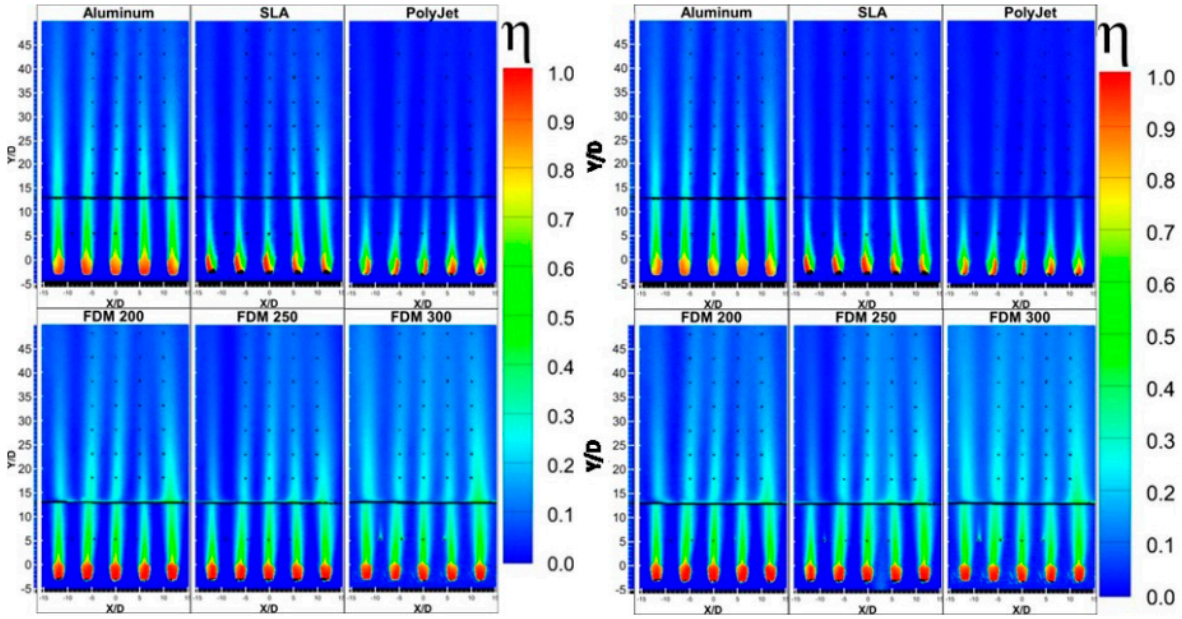

Figure 20. Effect of manufacturing techniques on the film cooling distribution [124]. More discussion is in [116].

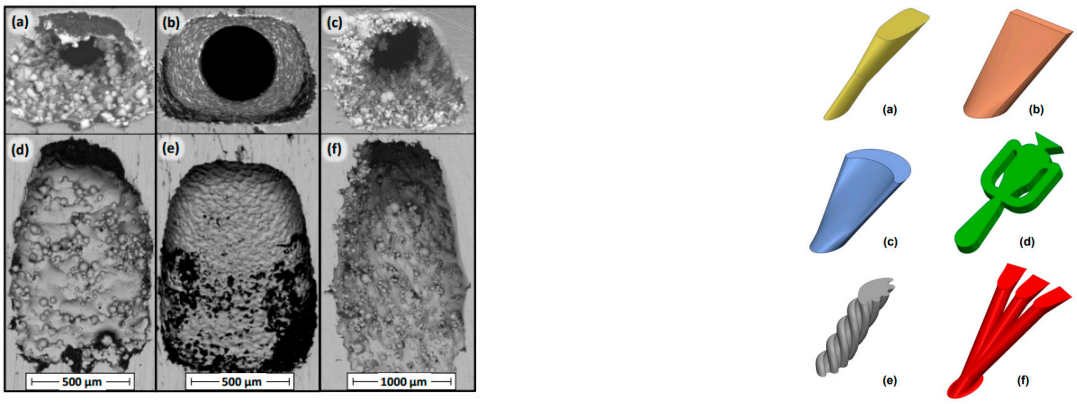

Figure 21. Microscopic surface roughness images of film cooling holes and innovative configurations (**a**) 7-7-7, (**b**) console, (**c**) crescent, (**d**) oscillator, (**e**) spiral and, (**f**) tripod [125]. More discussions are available in [121].

Overall, published literature suggests that the in-hole roughness is detrimental to film cooling downstream of the hole, but the in-hole convection is increased with increasing in-hole roughness, which can compete with decreasing film cooling and provide positive countereffect to improve the overall effectiveness in the vicinity of film holes. Since internal channel convection is positively affected by the channel roughness, the cooling affected zone (CAZ) by the film hole expands. Unfortunately, designers find that too cold CAZ increases thermal stress and can initiate cracks near the holes in the thermal barrier coating (TBC). It can be hypothesized that at the film hole exit, there is high heat transfer for the film coolant and keeping the target surface temperature lower in the vicinity of the hole exit may benefit the film performance. That is because a cooler metal temperature means lower heat pickup by the coolant at that location, but cooler metal is obtained by using coolant. What is the right balance of CAZ and film heat pickup can be an interesting topic for the researchers to investigate.

Research on the efficacy of additive manufacturing in film cooling performance is still in a nascent stage and relatively few numbers of studies have been conducted on engine-relevant scales and conditions. Full-scale turbine blades are being manufactured by the researchers using metal additive manufacturing technologies, and examples were shown in Figure 2 [13]. Several design constraints must be considered to ensure successful integration of film cooling holes in blade structures during additive manufacturing. The five decades of research signifies that the film cooling holes on a single airfoil can have varying orientations with varying cooling characteristics. Since heat load on an airfoil is not uniform, hole assignments in different regions of the airfoil become a control knob for the designers through AM. This control was not available prior to AM due to conventional manufacturing constraints. Note that Ni-Co alloys used for turbine components are tough to machine and some machine shops refer to them as "angry metals." Conventional drill breaks and milling tools deform when machining attempts are made on these alloys with simplistic machine tools. A correlation for film hole density based on local heat load and mechanical strength requirements will help the designers to obtain a rough estimate on total number of holes needed in a component.

Most investigations have been primarily conducted on flat plate-type coupons, but manufacturing holes on curved surfaces at varying angles can provide more realistic performance estimation. Moreover, why do we have to limit the feeder metering hole to straight and round? The metering hole can be curved and can help provide an exit coolant velocity profile that is beneficial to the local film cooling on the curved airfoil surface with vortex-strewn predictable but complex hot-gas flow. Shi et al. [126] studied the uncertainty from manufacturing deviations and observed 26% deviation in the discharge coefficient C_d. To the best of the authors' knowledge, there is no elaborate work conducted on additively manufactured compound holes and that can be analyzed in the near future. Also, the adiabatic film cooling effectiveness obtained through comparative analysis of polymeric coupons manufactured via nonmetal additive manufacturing technology can deviate from the actual performance of holes realized in metal via LPBF technologies unless comparable roughness scales are achieved. Even if the roughness scales are closely mimicked, another challenge is to quantify the heat transfer coefficient of these samples, as that cannot be overlooked for the overall cooling performance. The repeatability and reliability of the data obtained from additively manufactured film cooling coupons has to be ensured for wide-scale industrial applications. This can be done by having a set of correlations for robust relationships among AM process parameters, build direction orientation, final surface quality, and obtained flow and thermal properties on the samples. Despite the current challenges, the use of AM technologies is gaining traction and there is continuous effort by the researchers to optimize manufacturing processes for better gain and improved performance. This is definitely an active area for new inventions, such as those demonstrated in patents [33,34]. These patents indicate a cap element in the film hole, and influence of that is not yet available in the published literature. The knowledge base

on covered film holes is not yet publicly disclosed. AM technologies offer opportunities to bring such novel configurations in the mainstream applications.

Huang et al. [127] showed that imperfect holes can cause a decrease in film cooling effectiveness and at the same time decrease the coefficient of discharge for the same-sized hole. We would like to point out that a decrease in discharge coefficient allows for a bigger hole for the same throughput with a given pressure drop. That can be used as an advantage, as was discussed in opportunities found in impingement cooling [128].

5.3. AM Sweeping Film with Synthetic Jet (SJ)

A synthetic jet (SJ) is similar to the oscillator film as shown in Figure 21d. Figure 22 shows the layout and size variations that were tried in published literature. Recent developments on synthetic jet film cooling at the Ohio State University were published in several journal articles and in a dissertation [129–132]. Other notable publications can be found in Zhou et al. [133] and Kong et al. [134]. Zhou et al. used the SJ at the film exit and Kong et al. used SJ at the impingement configuration prior to the film exit. These studies showed the working principles of fluidic mechanisms and benefits of spreading the coolant towards better coverage.

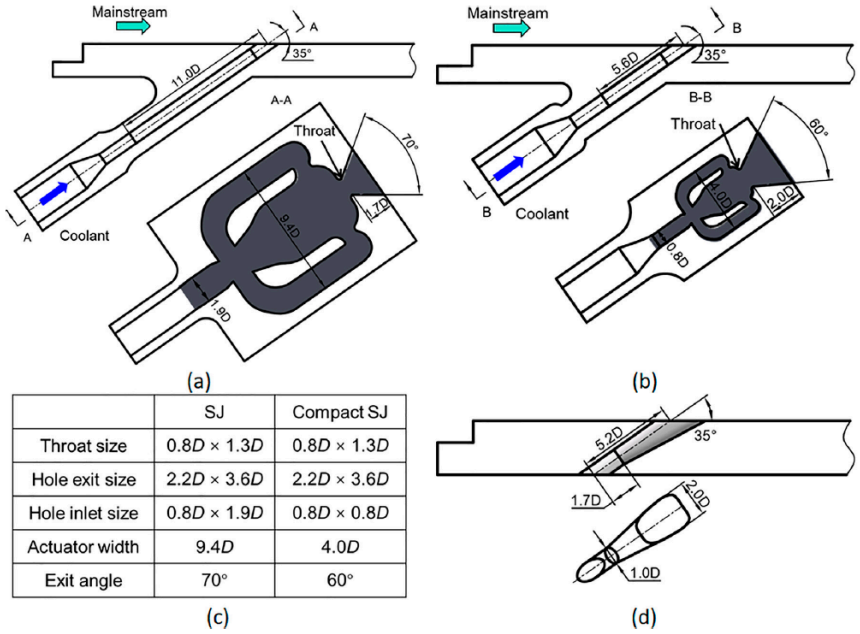

	SJ	Compact SJ
Throat size	0.8*D* × 1.3*D*	0.8*D* × 1.3*D*
Hole exit size	2.2*D* × 3.6*D*	2.2*D* × 3.6*D*
Hole inlet size	0.8*D* × 1.9*D*	0.8*D* × 0.8*D*
Actuator width	9.4*D*	4.0*D*
Exit angle	70°	60°

(c)

Figure 22. Synthetic Jet (SJ) and 7-7-7 holes used by Zhou et al. [133].

Figure 23 shows the inner mechanisms of the film development and stretching in z-direction. The oscillator size had a significant impact on the flow distribution and this work showed that more understanding and optimization processes are needed before a conclusively advantageous design can be obtained.

Figure 24 indicates that the film coverage is markedly better on the suction surface where the boundary layer is stretched thin due to hot-gas acceleration. Figure 25 shows the detailed film effectiveness distribution with SJ and regular shaped holes. The SJ film holes had a better spread but a smaller core peak. In a flat plate, the smaller core peak dissipated faster and as a result no significant benefits were observed with the SJ hole. In contrast to the flat plate, the suction side of an airfoil helps to hold the film longer towards the target surface and as a result the SJ film improved the performance in a curved configuration. Hossain et al. [132] showed the design and validation of SJ film concept in a direct metal laser sintered turbine nozzle guide vane and found that SJ is better for impinging the pressure side and SJ is better for film cooling in the suction side. The discharge from SJ and standard 7-7-7 holes were maintained to be similar and on average a 14% increase

in area-averaged film effectiveness was observed with SJ. An improvement of ~14% may be considered insignificant in emerging technologies, but in a mature technique like film cooling, this is a big achievement.

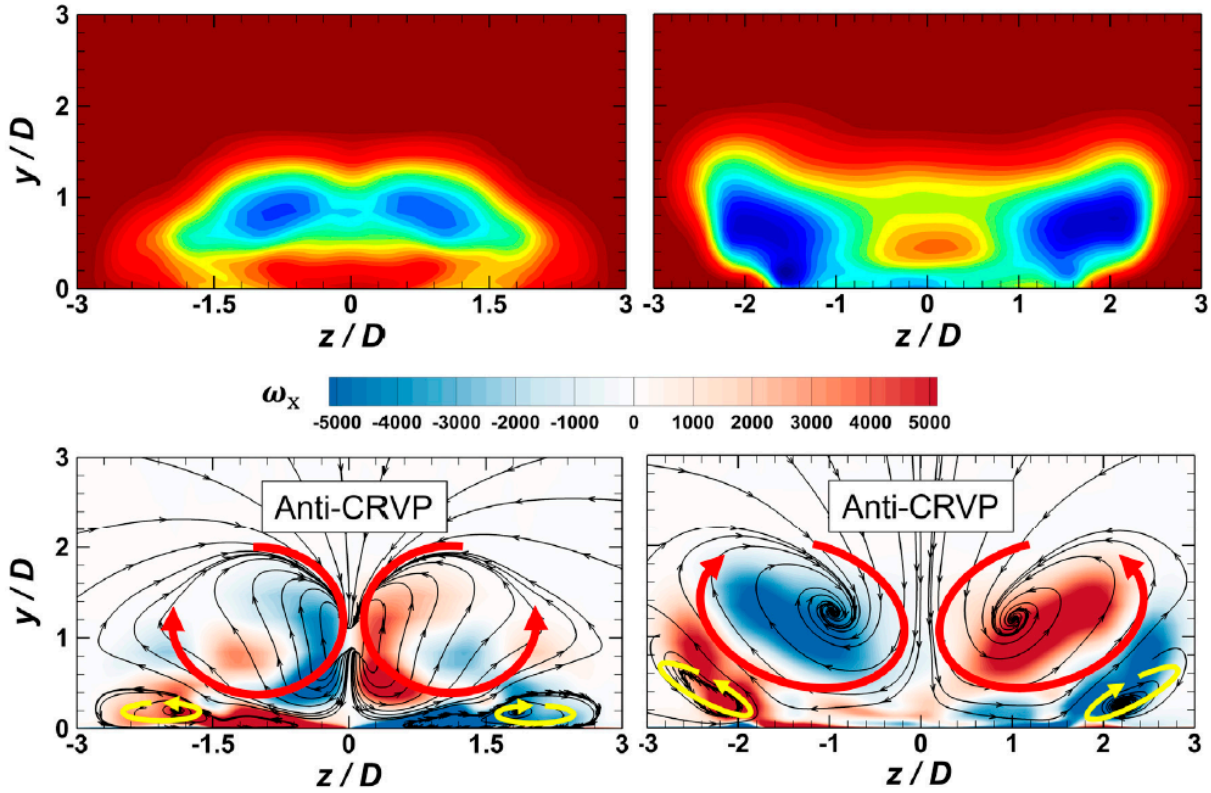

Figure 23. Sweeping effects from oscillating jets are demonstrated with two different SJ configurations [133].

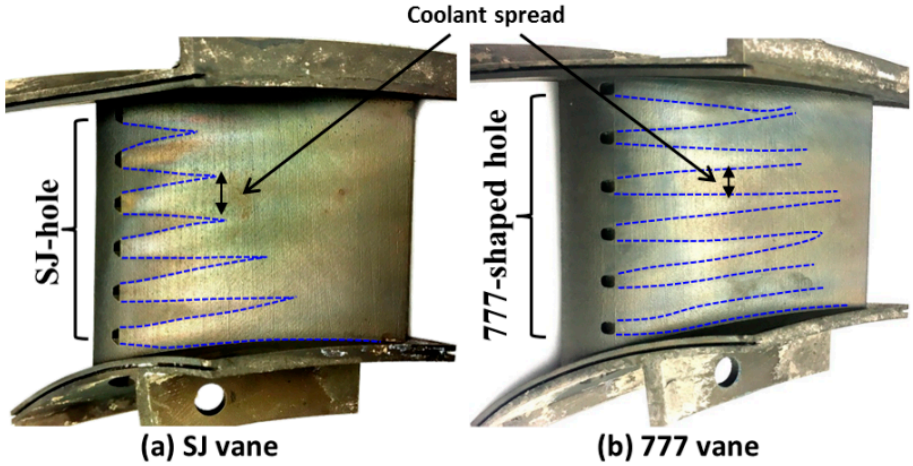

Figure 24. Synthetic jet hole coverage is much better than 777 film hole-pattern as reported by Hossain [130]. More discussion available in Hossain et al. [132].

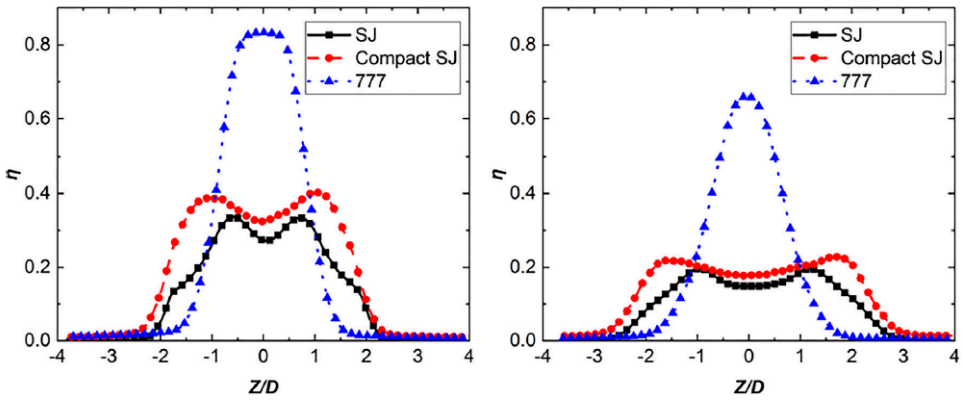

Figure 25. Synthetic jet configurations helped to spread the coolant on the target surface, as shown by the film effectiveness on a flat plate [133].

6. Future Challenges

New opportunities are continuously arising with the arrival of new technologies like pressure-gain combustor, ceramic composites, and hydrogen fuel. It is anticipated that gas turbine manufacturers are considering pressure-gain combustor (PGC) technology. A couple of open-access publications on pressure-gain combustion are referenced here for easier access [135,136]. Anand and Gutmark [137] showed that PGC is inherently transient and has rocket engine-like instabilities. Since film cooling is active in close proximity to the combustors, any transient flow or pulsing is bound to affect the film performance. Moreover, a gain in pressure in the combustor is bad for film discharge because the coolant air for the film is extracted prior to the combustor. The film discharge pressure difference assumed a pressure drop in the combustor and not a pressure gain. This increase in hot-gas pressure will require a pressure increase in the film coolant supply and that aspect has not been properly addressed yet. There is also a push to reduce the carbon-based fuel and the progress is being made towards using hydrogen in existing natural gas-fueled gas turbines. Chiesa et al. [138] showed that switching to hydrogen from natural gas involves more than just changing fuel lines. Hydrogen fuel can burn at a higher temperature with unacceptable NO_x emissions. As a result, the hydrogen combustion system uses significant amounts of dilution with steam or nitrogen. These additional flows can affect the existing film cooling systems and can be studied for future development. There are additional problems when ceramic–matrix composite (CMC) is used along with diluted hydrogen fuel. Steam is harmful to CMC [139] and a dry-air film is required to protect the CMC surface from the moisture containing combustion byproducts. The purpose of film in CMC is not primarily cooling; rather, it is about limiting hydrated degradation through a dry film layer, which opens up different types of opportunities for researchers and designers.

Opportunities in film cooling research that are beyond previous conventional research and can now be achieved with emerging AM technologies include:

- Hooded film holes
- Curved film holes
- Design alterations to accommodate AM roughness
- Adaptation of pressure-gain combustors
- Surface protection of CMC
- Adaptation for hydrogen fuel
- Pulsating and sweeping film
- Alterations in film hole inlet
- Film hole cooling affected zones
- Film hole density correlation with heat load and structural strength
- Manufacturing deviations and its impact
- Low discharge coefficient in larger rougher holes

7. Conclusions

Film cooling is essential in high-performance gas turbines and there is active research dedicated to improving film cooling technology. The ASME Turbo Expo 2022 conference had 10 presentations on film cooling. Primary developments in recently reported literature are in hole shapes, surface roughness, and hole arrangements; while controlling flow parameters were governed by density ratio, mass flux ratio, and momentum flux ratio. New cooling challenges are faced as hot-gas conditions became more severe. The operating factors challenging film cooling are higher gas temperature for better thermal efficiency, higher dump pressure (lower pressure difference across film hole inlet-to-outlet) due to pressure-gain combustors, and more curved airfoils as AM changes the core design process.

Fortunately, measurement techniques have improved and can provide inner details of the flow and heat transfer mechanisms to help improve the cooling design. The shaped exit film cooling holes have been shown to outperform basic cylindrical holes, but few studies suggest that the relative performance enhancement can be overestimated if the experiments were not conducted at engine-relevant freestream turbulence intensity conditions. Compound holes with orthogonal directional component to the hot gas tend to have higher adiabatic effectiveness, but that is accompanied by a higher heat transfer coefficient, which can diminish the overall performance of the film cooling. Shaped holes mitigate jet liftoff compared to cylindrical holes by reducing the momentum flux of the ejected fluid. The concept of the hooded film hole has not yet been studied in the published literature, but there are indications from the patent-publications that it is being privately evaluated.

Higher momentum flux with the same mass flow rate signifies higher unwanted penetration of ejected coolant into hot mainstream and subsequently causing more mixing, which usually results in lower film cooling effectiveness. Higher density ratio demonstrates delayed jet liftoff and obtains a higher overall effectiveness in general. Advective capacity ratio is being explored recently to scale the film cooling performance to engine-relevant conditions. This parameter needs to be further explored to confirm its suitability to scale performance over wide spectra of hole configurations and operating conditions. Experimental film cooling measurement techniques apply sophisticated mass transfer, transient liquid crystal thermography, and infrared imaging; with mass transfer techniques showing added advantage of reducing conduction errors, which are nearly unavoidable in heat-transfer based experiments. Pressure-sensitive paints, a type of mass transfer technique, has gained significant traction over the last two decades. These experimental techniques are complex and require years of training to measure thermal outcomes with acceptable accuracy.

Additive manufacturing is promising for cooling technologies because it helps build complex hole shapes (like synthetic jet oscillators) and customized configurations that are otherwise challenging or too expensive to build through conventional means. However, the few studies available on additively manufactured test coupons highlight inferior surface quality issues. The inherent roughness scales can be significant with respect to the hole diameters, and that can alter the mass flow rate and hence cooling performance. The in-hole roughness increases the in-hole convection but reduces film cooling effect due to increased momentum flux at the core of exiting jet. At similar flow conditions, additively manufactured film cooling coupons provided inferior overall effectiveness value than coupons with smoother EDM holes. The overall analysis suggests that surface characteristics cannot be ignored when characterizing film cooling performance of additively manufactured coupons along with other parameters discussed in the paper. The prospects of using additive manufacturing are promising and new shapes (not only for the film hole but also for the airfoil) and compound curved film hole configurations can be explored in the future. Film cooling technology in the context of emerging technologies like retrofitting existing gas turbines with hydrogen fuel combustors and new pressure-gain combustion systems are expected to initiate new research and development activities.

Author Contributions: I.K. wrote the primary content of the paper that was presented at the ASME conference. P.S. provided the guidance and necessary ingredients for the manuscript. S.D. took the lead on writing this modified journal article. All authors have read and agreed to the published version of the manuscript.

Funding: This research received no external funding.

Acknowledgments: The authors are thankful to their universities and the professional society ASME for the support provided to prepare this manuscript. Availability of illustrations and images from open access is also appreciated.

Conflicts of Interest: There are no conflict of interest.

Nomenclature

C	concentration
c_p	specific heat capacity (J/kg.K)
D	diameter of film cooling hole (m)
h	heat transfer coefficient (W/m^2.K)
I	momentum flux ratio
k	thermal conductivity of solid (W/m.K)
M	blowing ratio
P	partial pressure
q	heat flux (W/m^2)
t	time (s)
T	temperature (K)
Tu	turbulence intensity (%)
u	velocity (m/s)
x	streamwise distance

Greek letters

α	thermal diffusivity of solid (m^2/s)
ρ	density (kg/m^3)
η	adiabatic film effectiveness
ϕ	overall film effectiveness

Subscripts

aw	adiabatic wall temperature
c	coolant
i	initial/internal
ref	references
w	surface wall temperature
∞	mainstream
0	baseline case/no-coolant injection

Abbreviations

ACR	advective capacity ratio
AM	additive manufacturing
CAZ	cooling affected zone
CMC	ceramic–matrix composite
EDM	electro-discharge machining
FC	film cooling
FDM	fused deposition modeling

LPBF	laser powder bed fusion
PGC	pressure-gain combustor
SLM	selective laser melting
TBC	thermal barrier coating

References

1. Kaur, I.; Dutta, S.; Singh, P. A Review on Film Cooling Research: Historical Developments in Hole Shapes, Measurement Techniques, Effects of Operating Conditions, and Impact of Additive Manufacturing, HT2022-81803. In Proceedings of the ASME 2022 Heat Transfer Summer Conference, Philadelphia, PA, USA, 11–13 July 2022.
2. Bogard, D.G.; Thole, K.; Oliver, T. Integrated Turbine Component Cooling Designs Facilitated by Additive Manufacturing and Optimization. DOE-NETL. November 2021. Available online: https://netl.doe.gov/sites/default/files/netl-file/21UTSR_Bogard.pdf (accessed on 17 May 2022).
3. Wikipedia, Ultra High Temperature Ceramic Matrix Composite. Available online: https://en.wikipedia.org/wiki/Ultra_high_temperature_ceramic_matrix_composite (accessed on 22 May 2022).
4. Takashi, T.; Takeshi, N.; Kooun, T.; Takahito, A.; Tadashi, N. Research of CMC Application to Turbine Components. *IHI Eng. Rev.* **2005**, *38*, 2.
5. Lynch, S.; Hickner, M.; Frick, C.; Fertig, R. Development of Additive Manufacturing for Ceramic Matrix Composite Vanes. DE-FE0031758. February 2019. Available online: https://netl.doe.gov/sites/default/files/netl-file/20UTSR_Lynch.pdf (accessed on 22 May 2022).
6. Goldstein, R.J. Film Cooling. In *Advances in Heat Transfer*; Irvine, T.F., Hartnett, J.P., Eds.; Elsevier: Amsterdam, The Netherlands, 1971; Volume 7, pp. 321–379. [CrossRef]
7. Zhang, J.; Zhang, S.; Wang, C.; Tan, X. Recent Advances in Film Cooling Enhancement: A Review. *Chin. J. Aeronaut.* **2020**, *33*, 1119–1136. [CrossRef]
8. Grisson, W.M. *Liquid Film Cooling in Rocket Engines*; AEDC-TR-91-1; US Air Force: Washington, DC, USA, 1991.
9. Rao, M.P.; Biswal, P.; Prasad, B.V.S.S.S. A Computational Study of Mist Assisted Film Cooling. *Int. Commun. Heat Mass Transf.* **2018**, *95*, 33–41.
10. Hada, S.; Tsukagoshi, K.; Masada, J.; Ito, E. Test Results of the World's First 1600C J-Series Gas Turbine. *Mitsubishi Heavy Ind. Tech. Rev.* **2012**, *49*, 18–23.
11. Yuri, M.; Masada, J.; Tsukagoshi, K.; Ito, E.; Hada, S. Development of 1600C-Class High-Efficiency Gas Turbine for Power Generation Applying J-Type Technology. *Mitsubishi Heavy Ind. Tech. Rev.* **2013**, *50*, 3.
12. Horizon Technology. 3 Advantages & Disadvantages of Additive Manufacturing Processes vs. PM. 7 June 2021. Available online: https://www.horizontechnology.biz/blog/advantages-and-disadvantages-of-additive-manufacturing-process-vs-powder-metallurgy (accessed on 18 May 2022).
13. Magerramova, L.; Vasilyev, B.; Kinzburskiy, V. Novel Designs of Turbine Blades for Additive Manufacturing. In Proceedings of the Volume 5C: Heat Transfer, New York, NY, USA, 13–17 June 2016; p. V05CT18A001. [CrossRef]
14. Sotov, A.V.; Agapovichev, A.V.; Smelov, V.G.; Kokareva, V.V.; Dmitrieva, M.O.; Melnikov, A.A.; Golanov, S.P.; Anurov, Y.M. Investigation of the IN-738 Superalloy Microstructure and Mechanical Properties for the Manufacturing of Gas Turbine Engine Nozzle Guide Vane by Selective Laser Melting. *Int. J. Adv. Manuf. Technol.* **2020**, *107*, 2525–2535. [CrossRef]
15. Hanson, K. 3D-Printed Parts Made from Refractory Metals can Handle the Heat. *Additive Report*. Available online: https://www.thefabricator.com/additivereport/article/additive/3d-printed-parts-made-from-refractory-metals-can-handle-the-heat (accessed on 20 May 2022).
16. Stimpson, C.K.; Snyder, J.C.; Thole, K.A.; Mongillo, D. Effectiveness Measurements of Additively Manufactured Film Cooling Holes. *J. Turbomach.* **2017**, *140*, 011009. [CrossRef]
17. Keller, M.A.; Kloker, M.J. Direct Numerical Simulation of Foreign-Gas Film Cooling in Supersonic Boundary-Layer Flow. *AIAA J.* **2017**, *55*, 99–111. [CrossRef]
18. Chang, J.; Duan, X.; Du, Y.; Guo, B.; Pan, Y. Investigations on the Effect of Different Influencing Factors on Film Cooling Effectiveness under the Injection of Synthetic Coolant. *Sci. Rep.* **2021**, *11*, 1–14. [CrossRef]
19. Wang, C.; Fan, F.; Zhang, J.; Huang, Y.; Feng, H. Large Eddy Simulation of Film Cooling Flow from Converging Slot-Holes. *Int. J. Therm. Sci.* **2018**, *126*, 238–251. [CrossRef]
20. Han, J.C.; Dutta, S.; Ekkad, S. *Gas Turbine Heat Transfer and Cooling Technology*, 2nd ed.; CRC Press: New York, NY, USA, 2012.
21. Chen, Z.-Y.; Zhan, J.-M.; Li, C.-W.; Hu, W.-Q.; Gong, Y.-J. The Effect of Vortex Shedding in Film-Cooling Processes. *Heat Transf. Eng.* **2021**, *42*, 1432–1451. [CrossRef]
22. Huang, Y.; Zhang, J.-Z.; Wang, C.-H.; Zhu, X.-D. Multi-Objective Optimization of Laidback Fan-Shaped Film Cooling Hole on Turbine Vane Suction Surface. *Heat Mass Transf.* **2019**, *55*, 1181–1194. [CrossRef]
23. Mongillo, D.J., Jr.; Gleiner, M.S. Cooling Hole with Curved Metering Section. US 8850828 B2, 7 October 2014.
24. Li, H.M.; Ghaly, W.; Hassan, I. The Formation of Counter-Rotating Vortex Pair and the Nature of Liftoff-Reattachment in Film-Cooling Flow. *Fluids* **2016**, *1*, 39. [CrossRef]
25. Aminov, R.Z.; Moskalenko, A.B.; Kozhevnikov, A.I. Optimal Gas Turbine Inlet Temperature for Cyclic Operation. *IOP Conf. Ser. J. Phys.* **2018**, *1111*, 012046. [CrossRef]

26. Chen, A.F. Film Cooling with Forward and Backward Injection for Cylindrical and Fan-Shaped Holes Using PSP Measurement Technique. Ph.D. Thesis, Texas A&M University, College Station, TX, USA, 2013.
27. Park, S.P.; Jung, E.Y.; Kim, S.H.; Sohn, H.-S.; Cho, H.H. Enhancement of Film Cooling Effectiveness using Backward Injection Holes. *Int. J. Therm. Sci.* **2016**, *110*, 314–324. [CrossRef]
28. Barigozzi, G.; Abdeh, H.; Rouina, S.; Franchina, N. The Aero-Thermal Performance of Purge Flow and Discrete Holes Film Cooling of Rotor Blade Platform in Modern High Pressure Gas Turbines: A Review. *Int. J. Turbomach. Propuls. Power* **2022**, *7*, 22. [CrossRef]
29. Goldstein, R.J.; Eckert, E.R.G.; Burggraf, F. Effects of hole geometry and density on three-dimensional film cooling. *Int. J. Heat Mass Transf.* **1974**, *17*, 595–607. [CrossRef]
30. Bunker, R.S. A Review of Shaped Hole Turbine Film-Cooling Technology. *J. Heat Transf.* **2005**, *127*, 441–453. [CrossRef]
31. Narzary, D.P. Experimental Study of Gas Turbine Blade Film Cooling and Heat Transfer. Ph.D. Thesis, Texas A&M University, College Station, TX, USA, 2009. Available online: https://core.ac.uk/download/pdf/147135971.pdf (accessed on 28 August 2022).
32. Saumweber, C.; Schulz, A. Effect of Geometry Variations on the Cooling Performance of Fan-Shaped Cooling Holes. *J. Turbomach.* **2012**, *134*, 061008. [CrossRef]
33. Bunker, R.S. Additive Manufacturing Method for Making Complex Film Holes. US20170129014A1, 11 May 2017. Available online: https://patents.google.com/patent/US20170129014/en (accessed on 10 January 2022).
34. Dyson, T.E.; Gregg, J.R.; Rathay, N.W. Method of Forming Cooling Passage for Turbine Component with Cap Element. US10933481B2, 2 March 2021. Available online: https://patents.google.com/patent/US10933481B2/en (accessed on 10 January 2022).
35. Lee, S.I.; Jung, J.Y.; Song, Y.J.; Kwak, J.S. Effect of Mainstream Velocity on the Optimization of a Fan-Shaped Film-Cooling Hole on a Flat Plate. *Energies* **2021**, *14*, 3573. [CrossRef]
36. Hyams, D.; Leylek, J.H. A Detailed Analysis of Film Cooling Physics Part III: Streamwise Injection with Shaped Holes: 97-GT-271. In Proceedings of the ASME 1997 International Gas Turbine and Aeroengine Congress and Exhibition, Orlando, FL, USA, 2–5 June 1997.
37. Bogard, D.G.; Thole, K.A. Gas turbine film cooling. *J. Propuls. Power* **2006**, *22*, 249–270. [CrossRef]
38. Han, J.-C.; Ekkad, S. Recent Development in Turbine Blade Film Cooling. *Int. J. Rotating Mach.* **2001**, *7*, 21–40. [CrossRef]
39. Dupuy, D.; Perrot, A.; Odier, N.; Gicquel LY, M.; Duchaine, F. Boundary-Condition Models of Film-Cooling Holes for Large-Eddy Simulation of Turbine Vanes. *Int. J. Heat Mass Transf.* **2021**, *166*, 120763. [CrossRef]
40. Gritsch, M.; Schulz, A.; Wittig, S. Adiabatic Wall Effectiveness Measurements of Film-Cooling Holes with Expanded Exits. *J. Turbomach.* **1998**, *120*, 549–556. [CrossRef]
41. Schwarz, S.G.; Goldstein, R.J.; Eckert, E.R. The Influence of Curvature on Film Cooling Performance. *ASME J. Turbomach.* **1991**, *113*, 471–478. [CrossRef]
42. Walters, D.K.; Leylek, J.H. A Detailed Analysis of Film Cooling Physics: Part I- Streamwise Injection with Cylindrical Holes. *ASME J. Turbomach.* **2000**, *122*, 102–112. [CrossRef]
43. Baek, S.I.; Ahn, J. Large Eddy Simulation of Film Cooling with Triple Holes: Injectant Behavior and Adiabatic Film-Cooling Effectiveness. *Processes* **2020**, *8*, 1443. [CrossRef]
44. Li, W.; Lu, X.; Li, X.; Ren, J.; Jiang, H. Wall Thickness and Injection Direction Effects on Flat Plate Full-Coverage Film Cooling Arrays: Adiabatic Film Effectiveness and Heat Transfer Coefficient. *Int. J. Therm. Sci.* **2019**, *136*, 172–181. [CrossRef]
45. Kohil, A.; Bogard, D.G. Effects of Hole Shape on Film Cooling with Large Angle Injection. In Proceedings of the Volume 3: Heat Transfer; Electric Power; Industrial and Cogeneration, Indianapolis, IN, USA, 7–10 June 1999; p. V003T01A045. [CrossRef]
46. Sen, B.; Schmidt, D.L.; Bogard, D.G. Film Cooling with Compound Angle Holes: Heat Transfer. *J. Turbomach.* **1996**, *118*, 800–806. [CrossRef]
47. Gritsch, M.; Schulz, A.; Wittig, S. Film-Cooling Holes with Expanded Exits: Near-Hole Heat Transfer Coefficients. *Int. J. Heat Fluid Flow* **2000**, *21*, 146–155. [CrossRef]
48. Ligrani, P.M.; Ciriello, S.; Bishop, D.T. Heat Transfer, Adiabatic Effectiveness, and Injectant Distributions Downstream of a Single Row and Two Staggered Rows of Compound Angle Film-Cooling Holes. *J. Turbomach.* **1992**, *114*, 687–700. [CrossRef]
49. Haven, B.A.; Yamagata, D.K.; Kurosaka, M.; Yamawaki, S.; Maya, T. Anti-Kidney Pair of Vortices in Shaped Holes and Their Influence on Film Cooling Effectiveness: 97-GT-45. In Proceedings of the ASME Turbo Expo, Orlando, FL, USA, 2–5 June 1997.
50. Nasir, H.; Acharya, S.; Ekkad, S. Improved film cooling from cylindrical angled holes with triangular tabs: Effect of tab orientations. *Int. J. Heat Fluid Flow* **2003**, *24*, 657–668. [CrossRef]
51. Schmidt, D.L.; Sen, B.; Bogard, D.G. Film Cooling with Compound Angle Holes: Adiabatic Effectiveness. *J. Turbomach.* **1996**, *118*, 807–813. [CrossRef]
52. Schroeder, R.P.; Thole, K.A. Adiabatic Effectiveness Measurements for a Baseline Shaped Film Cooling Hole. In Proceedings of the ASME Turbo Expo 2014: Turbine Technical Conference and Exposition, Düsseldorf, Germany, 16–20 June 2014. [CrossRef]
53. Heidmann, J.D.; Ekkad, S. A Novel Antivortex Turbine Film-Cooling Hole Concept. *ASME J. Turbomach.* **2008**, *130*. [CrossRef]
54. Dhungel, A.; Lu, Y.; Phillips, W.; Ekkad, S.V.; Heidmann, J. Film Cooling from a Row of Holes Supplemented with Antivortex Holes. *J. Turbomach.* **2009**, *131*. [CrossRef]
55. Ramesh, S.; Ramirez, D.G.; Ekkad, S.V.; Alvin, M.A. Analysis of film cooling performance of advanced tripod hole geometries with and without manufacturing features. *Int. J. Heat Mass Transf.* **2016**, *94*, 9–19. [CrossRef]

56. Jung, E.Y.; Chung, H.; Choi, S.M.; Woo, T.-K.; Cho, H.H. Conjugate Heat Transfer on Full-Coverage Film Cooling with Array Jet Impingements with Various Biot Numbers. *Exp. Therm. Fluid Sci.* **2017**, *83*, 1–8. [CrossRef]
57. Ligrani, P.; Goodro, M.; Fox, M.; Moon, H.-K. Full-Coverage Film Cooling: Film Effectiveness and Heat Transfer Coefficients for Dense and Sparse Hole Arrays at Different Blowing Ratios. *ASME J. Turbomach.* **2012**, *134*. [CrossRef]
58. Metzger, D.E.; Takeuchi, D.I.; Kuenstler, P.A. Effectiveness and Heat Transfer with Full-Coverage Film Cooling. *J. Eng. Power* **1973**, *95*, 180–184. [CrossRef]
59. Ekkad, S.V.; Han, J.C.; Du, H. Detailed Film Cooling Measurements on a Cylindrical Leading Edge Model: Effect of Free-Stream Turbulence and Coolant Density. *ASME J. Turbomach.* **1998**, *120*, 799–807. [CrossRef]
60. Lu, Y.; Allison, D.; Ekkad, S.V. Turbine blade showerhead film cooling: Influence of hole angle and shaping. *Int. J. Heat Fluid Flow* **2007**, *28*, 922–931. [CrossRef]
61. Ramesh, S.; LeBlanc, C.; Narzary, D.; Ekkad, S.; Alvin, M.A. Film Cooling Performance of Tripod Antivortex Injection Holes Over the Pressure and Suction Surfaces of a Nozzle Guide Vane. *J. Therm. Sci. Eng. Appl.* **2017**, *9*. [CrossRef]
62. Ahn, J.; Schobeiri, M.T.; Han, J.-C.; Moon, H.-K. Effect of rotation on leading edge region film cooling of a gas turbine blade with three rows of film cooling holes. *Int. J. Heat Mass Transf.* **2007**, *50*, 15–25. [CrossRef]
63. Gao, Z.; Narzary, D.P.; Han, J.-C. Film cooling on a gas turbine blade pressure side or suction side with axial shaped holes. *Int. J. Heat Mass Transf.* **2008**, *51*, 2139–2152. [CrossRef]
64. Gao, Z.; Narzary, D.; Han, J.-C. Turbine Blade Platform Film Cooling with Typical Stator-Rotor Purge Flow and Discrete-Hole Film Cooling. *J. Turbomach.* **2009**, *131*. [CrossRef]
65. Narzary, D.P.; Liu, K.-C.; Rallabandi, A.P.; Han, J.-C. Influence of Coolant Density on Turbine Blade Film-Cooling Using Pressure Sensitive Paint Technique. *ASME J. Turbomach.* **2011**, *134*. [CrossRef]
66. Dutta, S.; Smith, R. Transfer Function Based Optimization of Film Hole Sizes with Conjugate Heat Transfer Analysis. In Proceedings of the ASME Turbo Expo 2020: Turbomachinery Technical Conference and Exposition, Virtual, 21–25 September 2020.
67. Smith, R.; Dutta, S. Conjugate thermal optimization with unsupervised machine learning. *J. Heat Transf.* **2021**, *143*, 052901. [CrossRef]
68. Pedersen, D.R.; Eckert, E.R.G.; Goldstein, R.J. Film Cooling with Large Density Differences Between the Mainstream and the Secondary Fluid Measured by the Heat-Mass Transfer Analogy. *ASME J. Heat Transf.* **1977**, *99*, 620–627. [CrossRef]
69. Sinha, A.; Bogard, D.; Crawford, M. Film-Cooling Effectiveness Downstream of a Single Row of Holes with Variable Density Ratio. *ASME J. Turbomach.* **1991**, *113*, 442–449. [CrossRef]
70. Yao, J.; Zhang, K.; Wu, J.; Lei, J.; Fang, Y.; Wright, L.M. An Experimental Investigation on Streamwise Distance and Density Ratio Effects on Double-Jet Film-Cooling. *Appl. Therm. Eng.* **2019**, *156*, 410–421. [CrossRef]
71. Ekkad, S.V.; Zapata, D.; Han, J.C. Film Effectiveness Over a Flat Surface With Air and CO2 Injection Through Compound Angle Holes Using a Transient Liquid Crystal Image Method. *J. Turbomach.* **1997**, *119*, 587–593. [CrossRef]
72. Johnson, B.; Tian, W.; Zhang, K.; Hu, H. An experimental study of density ratio effects on the film cooling injection from discrete holes by using PIV and PSP techniques. *Int. J. Heat Mass Transf.* **2014**, *76*, 337–349. [CrossRef]
73. Ekkad, S.; Han, J.-C. A Review of Hole Geometry and Coolant Density Effect on Film Cooling. In Proceedings of the ASME 2013 Heat Transfer Summer Conference, Minneapolis, MN, USA, 14–19 July 2013. [CrossRef]
74. Ito, S.; Goldstein, R.J.; Eckert, E.R.G. Film Cooling of a Gas Turbine Blade. *J. Eng. Power* **1978**, *100*, 476–481. [CrossRef]
75. Gartshore, S.S.; Salcudean, M.; Barnea, Y.; Zhang, K.; Aghadsi, F. Some Effects of Coolant Density on Film Cooling Effectiveness, 93-GT-76. In Proceedings of the ASME Turbo Expo, Cincinnati, OH, USA, 24–27 May 1993.
76. Eriksen, V.L.; Goldstein, R.J. Heat Transfer and Film Cooling Following Injection Through Inclined Circular Tubes. *ASME J. Heat Transf.* **1974**, *96*, 239–245. [CrossRef]
77. Ammari, H.D.; Hay, N.; Lampard, D. The Effect of Density Ratio on the Heat Transfer Coefficient from a Film-Cooled Flat Plate. *ASME J. Turbomach.* **1990**, *96*, 444–450. [CrossRef]
78. Li, W.; Lu, X.; Li, X.; Ren, J.; Jiang, H. High Resolution Measurements of Film Cooling Performance of Simple and Compound Angle Cylindrical Holes with Varying Hole Length-to-Diameter Ratio- Part I: Adiabatic Film Effectiveness. *Int. J. Therm. Sci.* **2018**, *124*, 146–161. [CrossRef]
79. Colban, W.F. *A Detailed Study of Fan-Shaped Film-Cooling for a Nozzle Guide Vane for an Industrial Gas Turbine*; Virginia Polytechnic Institute and State University: Blacksburg, VA, USA, 2005. Available online: https://vtechworks.lib.vt.edu/bitstream/handle/10919/29856/ETD_Colban.pdf?sequence=1 (accessed on 12 September 2022).
80. Schmidt, D.L.; Bogard, D.G. Effects of Free-Stream Turbulence and Surface Roughness on Film Cooling. In Proceedings of the Volume 4: Heat Transfer; Electric Power; Industrial and Cogeneration, Birmingham, UK, 10–13 June 1996. [CrossRef]
81. Fischer, J.P.; McNamara, L.J.; Rutledge, J.L.; Polanka, M.D. Scaling Flat-Plate, Low-Temperature Adiabatic Effectiveness Results Using the Advective Capacity Ratio. *ASME J. Turbomach.* **2020**, *142*, 1–33. [CrossRef]
82. Rutledge, J.L.; Polanka, M.D. Computational Fluid Dynamics Evaluations of Unconventional Film Cooling Scaling Parameters on a Simulated Turbine Blade Leading Edge. *ASME J. Turbomach.* **2014**, *136*. [CrossRef]
83. Saumweber, C.; Schulz, A. Free-Stream Effects on the Cooling Performance of Cylindrical and Fan-Shaped Cooling Holes. *ASME J. Turbomach.* **2012**, *134*, 061007. [CrossRef]
84. Han, J.-C.; Rallabandi, A. Turbine blade film cooling using PSP technique. *Front. Heat Mass Transf. (FHMT)* **2010**, *1*. [CrossRef]

85. Goldstein, R.J.; Jin, P. Film Cooling Downstream of a Row of Discrete Holes with Compound Angle. *ASME J. Turbomach.* **2000**, *123*, 222–230. [CrossRef]
86. Kwak, J.S.; Han, J.-C. Heat Transfer Coefficients and Film-Cooling Effectiveness on a Gas Turbine Blade Tip. *ASME J. Heat Transf.* **2003**, *125*, 494–502. [CrossRef]
87. Ekkad, S.V.; Ou, S.; Rivir, R.B. A Transient Infrared Thermography Method for Simultaneous Film Cooling Effectiveness and Heat Transfer Coefficient Measurements from a Single Test. *ASME J. Turbomach.* **2004**, *126*, 597–603. [CrossRef]
88. Vedula, R.J.; Metzger, D.E. A method for the simultaneous determination of local effectiveness and heat transfer distributions in three-temperature convection situations. In Proceedings of the ASME International Gas Turbine and Aeroengine Congress and Exposition, Orlando, FL, USA, 3–6 June 1991.
89. Bitter, M.; Hilfer, M.; Schubert, T.; Klein, C.; Niehuis, R. An Ultra-Fast TSP on a CNT Heating Layer for Unsteady Temperature and Heat Flux Measurements in Subsonic Flows. *Sensors* **2022**, *22*, 657. [CrossRef]
90. Zhang, L.J.; Jaiswal, R.S. Turbine Nozzle Endwall Film Cooling Study Using Pressure-Sensitive Paint. *ASME J. Turbomach.* **2001**, *123*, 730–738. [CrossRef]
91. Wright, L.M.; Gao, Z.; Varvel, T.A.; Han, J.-C. Assessment of steady state PSP, TSP, and IR measurement techniques for flat plate film cooling. In Proceedings of the Heat Transfer Summer Conference, San Francisco, CA, USA, 17–22 July 2005; Volume 47330, pp. 37–46.
92. Russin, R.A.; Alfred, D.; Wright, L.M. Measurement of Detailed Heat Transfer Coefficient and Film Cooling Effectiveness Distributions Using PSP and TSP. In Proceedings of the ASME Turbo Expo 2009: Power for Land, Sea, and Air, Orlando, FL, USA, 8–12 June 2009; Volume GT2009-59975. [CrossRef]
93. Shiau, C.-C.; Chowdhury, N.H.K.; Yang, S.-F.; Han, J.-C.; MirzaMoghadam, A.; Riahi, A. Heat Transfer Coefficients and Film Cooling Effectiveness of Transonic Turbine Vane Suction Surface Using TSP Technique GT2016-56264. In Proceedings of the ASME Turbo Expo 2016: Turbomachinery Technical Conference and Exposition, Seoul, Korea, 13–17 June 2016.
94. Gao, Z.; Han, J.-C. Influence of Film-Hole Shape and Angle on Showerhead Film Cooling Using PSP Technique. *ASME J. Heat Transf.* **2009**, *131*, 061701. [CrossRef]
95. Li, S.-J.; Yang, S.-F.; Han, J.-C. Effect of Coolant Density on Leading Edge Showerhead Film Cooling Using the Pressure Sensitive Paint Measurement Technique. *ASME J. Turbomach.* **2014**, *136*, 051011. [CrossRef]
96. Ahn, J.; Schobeiri, M.T.; Han, J.-C.; Moon, H.-K. Film Cooling Effectiveness on the Leading Edge Region of a Rotating Turbine Blade with Two Rows of Film Cooling Holes Using Pressure Sensitive Paint. *ASME J. Heat Transf.* **2006**, *128*, 879–888. [CrossRef]
97. Rallabandi, A.P.; Li, S.-J.; Han, J.-C. Unsteady Wake and Coolant Density Effects on Turbine Blade Film Cooling Using Pressure Sensitive Paint Technique. *ASME J. Heat Transf.* **2012**, *134*, 081701. [CrossRef]
98. Qin, Y.; Chen, P.; Ren, J.; Jiang, H. Effects of Wall Curvature and Streamwise Pressure Gradient on Film Cooling Effectiveness. *Appl. Therm. Eng.* **2016**, *107*, 776–784. [CrossRef]
99. Bunker, R.S. The Effects of Manufacturing Tolerances on Gas Turbine Cooling. *ASME J. Turbomach.* **2009**, *131*, 041018. [CrossRef]
100. Marimuthu, S.; Smith, B. Water-jet guided laser drilling of thermal barrier coated aerospace alloy. *Int. J. Adv. Manuf. Technol.* **2021**, *113*, 177–191. [CrossRef]
101. Bons, J.P.; Taylor, R.P.; McClain, S.T.; Rivir, R.B. The Many Faces of Turbine Surface Roughness. In Proceedings of the Volume 3: Heat Transfer; Electric Power; Industrial and Cogeneration, New Orleans, LA, USA, 4–7 June 2001. [CrossRef]
102. Bogard, D.G.; Schmidt, D.L.; Tabbita, M. Characterization and Laboratory Simulation of Turbine Airfoil Surface Roughness and Associated Heat Transfer. In Proceedings of the ASME 1996 International Gas Turbine and Aeroengine Congress and Exhibition, Birmingham, UK, 10–13 June 1996. [CrossRef]
103. Chen, X.; Long, Y.; Wang, Y.; Weng, S.; Luan, Y. Large Eddy Simulation of Film Cooling from Cylindrical Holes Partially Blocked by CaO-MgO-Al_2O_3-SiO_2. *Int. Commun. Heat Mass Transf.* **2021**, *129*. [CrossRef]
104. Schroeder, R.P.; Thole, K.A. Effect of In-Hole Roughness on Film Cooling from a Shaped Hole. *ASME J. Turbomach.* **2016**, *139*. [CrossRef]
105. Zamiri, A.; You, S.J.; Chung, J.T. Surface Roughness Effects on Film-Cooling Effectiveness in a Fan-Shaped Cooling Hole. *Aerosp. Sci. Technol.* **2021**, *119*. [CrossRef]
106. Zamiri, A.; Barigozzi, G.; Chung, J.T. Large Eddy Simulation of Film Cooling Flow from Shaped Holes with Different Geometrical Parameters. *Int. J. Heat Mass Transf.* **2022**, *196*. [CrossRef]
107. Goldstein, R.J.; Eckert, E.R.G.; Chiang, H.D.; Elovic, E. Effect of Surface Roughness on Film Cooling Performance. *J. Eng. Gas Turbines Power* **1985**, *107*, 111–116. [CrossRef]
108. McMasters, M.A.; Benjamin, M.A.; Mancini, A.; Lohmueller, S.J. Fuel Nozzle. Patent US008806871B2, 18 August 2014.
109. Benjamin, M.A.; Mook, J.T.; Henderson, S.J.; Martinez, R. Fuel Nozzle Structure for Air Assist Injection. Patent US2017000303A1, 5 January 2017.
110. Korber, R. Aerodynamic Film Cooling Holes. Available online: https://www.kit-technology.de/en/technology-offers/details/689 (accessed on 28 August 2022).
111. Fraas, M. Offenlegungsschrift. Patent. Available online: https://www.kit-technology.de/fileadmin/user_upload/DE102018108729A1.pdf (accessed on 28 August 2022).
112. Fraas Marc Glasenapp, T.; Schulz, A.; Bauer, H.-J. Optimized Inlet Geometry of a Laidback Fan-Shaped Film Cooling Hole-Experimental Study of Film Cooling Perfromance. *Int. J. Heat Mass Transf.* **2019**, *128*, 980–990. [CrossRef]

113. Research Project Explores Mass Surface Finishing for Metal AM Parts. *Metal AM*, 18 May 2020. Available online: https://www.metal-am.com/research-project-explores-mass-surface-finishing-for-metal-am-parts/ (accessed on 28 August 2022).
114. Townsend, A.; Senin, N.; Blunt, L.; Leach, R.K.; Taylor, J.S. Surface Texture Metrology for Metal Additive Manufacturing: A Review. *Precis. Eng.* **2016**, *46*, 34–37. [CrossRef]
115. Dutta, S.; Dasgupta, S.; Chimata, G. Engineering and Economic Aspects of Additive Manufacturing in Energy Related Industries. 2020. Available online: https://engrxiv.org/preprint/view/1222/ (accessed on 20 May 2022).
116. Aghasi, P.; Gutmark, E.; Munday, D. Dependence of Film Cooling Effectiveness on 3D Printed Cooling Holes. *ASME J. of Heat Transfer* **2017**. HT-16-1577. [CrossRef]
117. Shi, W.; Li, X.; Wang, L.; Ren, J.; Jiang, H. Large Eddy Simulation of Film Cooling for the Real Additive Manufactured Fan-Shaped Holes. In Proceedings of the ASME Turbo Expo 2020: Turbomachinery Technical Conference and Exposition, Virtual, 21–25 September 2020; Volume 84171, p. V07BT12A036.
118. Lee, S.; Hwang, W.; Yee, K. Robust design optimization of a turbine blade film cooling hole affected by roughness and blockage. *Int. J. Therm. Sci.* **2018**, *133*, 216–229. [CrossRef]
119. Salvadori, S.; Carnevale, M.; Fanciulli, A.; Montomoli, F. Uncertainty Quantification of Non-Dimensional Parameters for a Film Cooling Configuration in Supersonic Conditions. *Fluids* **2019**, *4*, 155. [CrossRef]
120. Stimpson, C.K.; Snyder, J.C.; Thole, K.A.; Mongillo, D. Effects of coolant feed direction on additively manufactured film cooling holes. *ASME J. Turbomach.* **2018**, *140*, 111001. [CrossRef]
121. Snyder, J.C.; Thole, K.A. Performance of Public Film Cooling Geometries Produced Through Additive Manufacturing. *ASME J. Turbomach.* **2020**, *142*, 1–30. [CrossRef]
122. Dutta, S.; Smith, R. Nonlinear Optimization of Turbine Conjugate Heat Transfer with Iterative Machine Learning and Training Sample Replacement. *Energ. J.* **2020**, *13*, 4587. [CrossRef]
123. Vinton, K.R.; Nahang-Toudeshki, S.; Wright, L.M.; Carter, A. Full Coverage Film Cooling Performance for Combustor Cooling Manufactured Using DMLS. In Proceedings of the ASME Turbo Expo 2016: Turbomachinery Technical Conference and Exposition, Seoul, Korea, 13–17 June 2016. [CrossRef]
124. Aghasi, P. Dependence of Film Cooling Effectiveness on 3D Printed Cooling Holes. Master's Thesis, University of Cincinnati, Cincinnati, OH, USA, 2016.
125. Snyder, J.C. Improving Turbine Cooling through Control of Surface Roughness in the Additive Manufacturing Process. Ph.D. Thesis, The Pennsylvania State University, State College, PA, USA, 2019. Available online: https://etda.libraries.psu.edu/files/final_submissions/18773 (accessed on 28 August 2022).
126. Shi, W.; Chen, P.; Li, X.; Ren, J.; Jiang, H. Uncertainty Quantification of the Effects of Small Manufacturing Deviations on Film Cooling: A Fan-Shaped Hole. *Aerospace* **2019**, *6*, 46. [CrossRef]
127. Huang, K.; Zhang, J.; Tan, X.; Shan, Y. Experimental Study on Film Cooling Performance of Imperfect Holes. *Chin. J. Aeronaut.* **2018**, *31*, 1215–1221. [CrossRef]
128. Dutta, S.; Singh, P. Opportunities in Jet-Impingement Cooling for Gas-Turbine Engines. *Energies* **2021**, *14*, 6587. [CrossRef]
129. Hossain, M.A.; Agricola, L.; Ameri, A.; Gregory, J.W.; Bons, J.P. Sweeping Jet Film Cooling on a Turbine Vane. *ASME J. Turbomach.* **2019**, *141*, 031007. [CrossRef]
130. Hossain, M.A.; The Ohio State University. Sweeping Jet Film Cooling. 2020. Available online: https://etd.ohiolink.edu/apexprod/rws_etd/send_file/send?accession=osu1586462423029754&disposition=inline (accessed on 11 July 2022).
131. Hossain, M.A.; Ameri, A.; Gregory, J.W.; Bons, J.P. Sweeping Jet Film Cooling at High Blowing Ratio on a Turbine Vane. *ASME J. Turbomach.* **2020**, *142*, 58653. [CrossRef]
132. Hossain, M.A.; Ameri, A.; Gregory, J.W.; Bons, J.P. Experimental Investigation of Innovative Cooling Schemes on an Additively Manufactured Engine Scale Turbine Nozzle Guide Vane. *ASME J. Turbomach.* **2021**, *143*, 1–39. [CrossRef]
133. Zhou, W.; Wang, K.; Yuan, T. Spatiotemporal Distributions of Sweeping Jet Film Cooling with a Compact Geometry. *Phys. Fluids* **2022**, *34*. [CrossRef]
134. Kong, X.; Zhang, Y.; Li, G.; Lu, X.; Zhu, J.; Xu, J. Numerical Simulation of the Flow and Heat Transfer Characteristics of Sweeping and Direct Jets on a Flat Plate with Film Holes. *Energies* **2022**, *15*, 4470. [CrossRef]
135. Neumann, N.; Peitsch, D. Potentials for Pressure Gain Combustion in Advanced Gas Turbine Cycles. *Appl. Sci.* **2019**, *9*, 3211. [CrossRef]
136. Stathopoulos, P. Comprehensive Thermodynamic Analysis of the Humphrey Cycle for Gas Turbines with Pressure Gain Combustion. *Energies* **2018**, *11*, 3521. [CrossRef]
137. Anand, V.; Gutmark, E. Rotating Detonation Combustors and Their Similarities to Rocket Instabilities. *Prog. Energy Combust. Sci.* **2019**, *73*, 182–234. [CrossRef]
138. Chiesa, P.; Lozza, G.; Mazzocchi, L. Using Hydrogen as Gas Turbine Fuel. *ASME J. Eng. Gas Turbines Power* **2005**, *127*, 73–80. [CrossRef]
139. Mall, S.; Ryba, J.L. Effects of Moisture on Tensile Stress Rupture Behavior of a SiC/SiC Composite at Elevated Temperatures. *Compos. Sci. Technol.* **2008**, *68*, 274–282. [CrossRef]